Integrated system for temperature-controlled fast protein liquid chromatography. II. Optimized adsorbents and ‘single column continuous operation’

Cao, Ping; Müller, Tobias K.h.; Ketterer, Benedikt; Ewert, Stephanie; Theodosiou, Eirini; Thomas, Owen R.T.; Franzreb, Matthias

DOI:
10.1016/j.chroma.2015.05.039

Document Version
Peer reviewed version

Citation for published version (Harvard):
Cao, P, Müller, TKH, Ketterer, B, Ewert, S, Theodosiou, E, Thomas, ORT & Franzreb, M 2015, 'Integrated system for temperature-controlled fast protein liquid chromatography. II. Optimized adsorbents and ‘single column continuous operation'', *Journal of Chromatography A*, vol. 1403, pp. 118-131. https://doi.org/10.1016/j.chroma.2015.05.039

Accepted Manuscript

Title: Integrated system for temperature-controlled fast protein liquid chromatography. II. Optimized adsorbents and 'single column continuous operation'

Author: Ping Cao Tobias K.H. Müller Benedikt Ketterer Stephanie Ewert Eirini Theodosiou Owen R.T. Thomas Matthias Franzreb

PII: S0021-9673(15)00732-3
DOI: http://dx.doi.org/doi:10.1016/j.chroma.2015.05.039
Reference: CHROMA 356520

To appear in: *Journal of Chromatography A*

Received date: 29-3-2015
Revised date: 13-5-2015
Accepted date: 15-5-2015

Please cite this article as: P. Cao, T.K.H. Müller, B. Ketterer, S. Ewert, E. Theodosiou, O.R.T. Thomas, M. Franzreb, Integrated system for temperature-controlled fast protein liquid chromatography. II. Optimized adsorbents and 'single column continuous operation', *Journal of Chromatography A* (2015), http://dx.doi.org/10.1016/j.chroma.2015.05.039

- Three beaded agarose media are grafted with networks of temperature sensitive anionic copolymers.
- Base matrix X-linking chemistry is shown to strongly influence the grafted copolymer composition.
- Travelling Cooling Zone Reactor chromatography uses a single column operated isocratically.
- Small diameter wide pored supports are best suited for protein separations in TCZR chromatography.
- TCZR chromatography can continuously accumulate, concentrate and fractionate proteins.

Integrated system for temperature-controlled fast protein liquid chromatography. II. Optimized adsorbents and 'single column continuous operation'

Ping Cao[a,3] Tobias K.H. Müller[b,1,3], Benedikt Ketterer[b], Stephanie Ewert[a,b], Eirini Theodosiou[a,2], Owen R.T. Thomas[a,*], Matthias Franzreb[b,**]

[a]School of Chemical Engineering, College of Engineering and Physical Sciences, University of Birmingham, Edgbaston, Birmingham B15 2TT, England, UK

[b]Institute for Functional Interfaces, Karlsruhe Institute of Technology, Hermann-von-Helmholtz-Platz 1, 76344 Eggenstein-Leopoldshafen, Germany

*Corresponding author. Tel. +44 121 414578; fax: +44 121 4145377.

**Corresponding author. Tel.: +49 721 608 23595; fax: +49 721 608 23478

E-mail addresses: o.r.t.thomas@bham.ac.uk (O.R.T. Thomas); matthias.franzreb@kit.edu (M. Franzreb).

[1] Present address: Evonik Industries AG, Rodenbacher Chausee 4, 63457 Hanau, Germany

[2] Present address: Department of Chemical Engineering, School of Aeronautical, Automotive, Chemical and Materials Engineering, Loughborough University, Loughborough LE11 3TU, UK

[3] These authors contributed equally to the experimental work in this study

Abstract

Continued advance of a new temperature-controlled chromatography system, comprising a column filled with thermoresponsive stationary phase and a travelling cooling zone reactor (TCZR), is described. Nine copolymer grafted thermoresponsive cation exchangers(thermoCEX) with different balances of thermoresponsive (*N*-isopropylacrylamide), hydrophobic *(N-tert*-butylacrylamide) and negatively charged (acrylic acid) units were fashioned from three cross-linked agarose media differing in particle size and pore dimensions. Marked differences in grafted copolymer composition on finished supports were sourced to base matrix hydrophobicity. In batch binding tests with lactoferrin, maximum binding capacity (q_{max}) increased strongly as a function of charge introduced, but became increasingly independent of temperature, as the ability of the tethered copolymer networks to switch between extended and collapsed states was lost. ThermoCEX formed from Sepharose CL-6B (A2), Superose 6 Prep Grade (B2) and Superose 12 Prep Grade (C1) under identical conditions displayed the best combination of thermoresponsiveness ($q_{max,50°C}$ / $q_{max,10°C}$ ratios of 3.3, 2.2 and 2.8 for supports 'A2', 'B2' and 'C1' respectively) and lactoferrin binding capacity ($q_{max,50°C}$ ~56, 29 and 45 mg/g for supports 'A2', 'B2' and 'C1' respectively), and were selected for TCZR chromatography. With the cooling zone in its parked position, thermoCEX filled columns were saturated with lactoferrin at a binding temperature of 35 °C, washed with equilibration buffer, before initiating the first of 8 or 12 consecutive movements of the cooling zone along the column at 0.1 mm/s. A reduction in particle diameter (A2 ➞ B2) enhanced lactoferrin desorption, while one in pore diameter (B2 ➞ C1) had the opposite effect. In subsequent TCZR experiments conducted with thermoCEX 'B2' columns continuously fed with lactoferrin or 'lactoferrin + bovine serum albumin' whilst simultaneously moving the cooling zone, lactoferrin was intermittently concentrated at regular intervals within the exiting flow as sharp uniformly sized peaks. Halving the lactoferrin feed concentration to 0.5 mg/mL, slowed acquisition of steady state, but increased

the average peak concentration factor from 7.9 to 9.2. Finally, continuous TCZR mediated separation of lactoferrin from bovine serum albumin was successfully demonstrated. While the latter's presence did not affect the time to reach steady state, the average lactoferrin mass per peak and concentration factor both fell (respectively from 30.7 to 21.4 mg and 7.9 to 6.3), and lactoferrin loss in the flowthrough between elution peaks increased (from 2.6 to 12.2 mg). Fouling of the thermoCEX matrix by lipids conveyed into the feed by serum albumin is tentatively proposed as responsible for the observed drops in lactoferrin binding and recovery.

Keywords: Copolymer modified agarose adsorbents; Ion exchange adsorption; Lower critical solution temperature (LCST); *N*-isopropylacrylamide; Smart polymers; Travelling cooling zone reactor

1. Introduction

Today, liquid chromatography is universally recognized as a supremely effective and practical bioseparation tool [1,2]. There are a multitude of reasons for this, but perhaps the two most important are the technique's adaptability to analytical and preparative separation tasks [3] and the availability of a huge variety of differently functionalized chromatographic supports affording orthogonal separation mechanisms [4,5]. In typical adsorption chromatography, defined amounts of a given feed solution, containing a single target component and multiple contaminants, are loaded onto a fixed-bed of adsorbent contained in a chromatography column. While the target component adsorbs, to be recovered in a later dedicated elution step by changing the chemical composition of the mobile phase, contaminant species either flow through the column unhindered, or alternatively are washed out in a subsequent washing step and/or during elution procedures. In addition to modifying the mobile phase's chemical composition, physical parameters can also be manipulated to influence protein adsorption to and desorption from chromatographic supports; the most popular of these being temperature, especially in the case of Hydrophobic Interaction Chromatography, HIC [6-10]. According to the Gibbs-Helmholtz equation, an increase in temperature exerts an influence similar to that imposed by raising the cosmotropic salt content in the mobile phase during HIC, which leads to enhanced protein adsorption affinity [8]. However, the relatively small differences in working capacity, even across temperature differentials as high as 40 °C, makes HIC adsorbents unattractive materials for purely temperature mediated liquid chromatography. The anchoring of 'smart' temperature–sensitive polymers or 'smart' thermoresponsive polymers onto chromatography supports offers a potential means of overcoming this drawback.

Smart thermoresponsive polymers are ones that exhibit inverse temperature solubility behaviour, i.e. they are water-soluble at low temperature and insoluble at high temperature, above a critical temperature known as the lower critical solution temperature (LCST) [11].

The most studied smart thermoresponsive polymer by far is poly(*N*-isopropylacrylamide) or pNIPAAm [12-14], and it's successful and broad application within biomedicine and biotechnology is extensively documented [15-18]. pNIPAAm undergoes a sharp reversible 'hydrophilic coil – hydrophobic globule' phase transition in water at an LCST of 32–34 ºC [12,13]. A large body of work on endowing chromatographic packing materials with temperature switchable behavior, through their modification with e.g. pNIPAAm or pNIPAAm copolymers, has appeared since the 1990s [19-24]. Most of this has involved modification of small pored inorganic or hydrophobic (polystyrene based) chromatography supports for use in analytical separations of small biomolecules (especially steroids). In stark contrast, very little has been done on the modification of softer macroporous media for preparative separations of much larger macromolecules, such as proteins. [22-24]. Maharjan et al. [22] and subsequently we [23] grafted lightly cross-linked networks of poly(*N*-isopropylacrylamide-*co*-*N*-tert-butylacrylamide-*co*-acrylic acid) into the surfaces of cross-linked agarose supports to produce thermoresponsive cation exchangers (hereafter abbreviated to thermoCEX). In tests with the thermally robust protein lactoferrin (LF) and jacketed columns of thermoCEX media, LF previously adsorbed at a higher temperature could be desorbed by lowering the mobile phase and column temperature.

To exploit thermoresponsive chromatography media more effectively, we invented a bespoke column arrangement [23], the so-called Travelling Cooling Zone Reactor (TCZR). TCZR chromatography employs a vertically held stainless steel walled column filled with thermoresponsive stationary phase and a computer-controlled motor-driven Peltier cooling device (the travelling cooling zone, TCZ) surrounding a discrete zone of the column (Fig. 1). In standard operation, a protein feed is administered to the column at an elevated temperature. On completion of the loading phase, the column is irrigated with an equilibration buffer whilst simultaneously moving the TCZ along the full length of the separation column

(multiple times) in the direction of the mobile phase, and at a velocity lower than that of the interstitial fluid. With each TCZ arrival at the end of the column, a sharp concentrated protein peak appears in the exiting flow, which can be collected by means of a fraction collector.

In this second follow up study, we push the boundaries of the TCZR chromatography concept further. From 3 different agarose base matrices, we construct and fully characterize 9 thermoCEX media varying in particle size, pore diameter, and copolymer composition, and subsequently identify, from batch adsorption and batch mode TCZR chromatography, the thermoCEX variant best suited for operation in TCZR modified columns. We then demonstrate, for the first time, how TCZR can be operated in continuous mode, to accumulate and concentrate a model binding protein (LF), and then separate the same target molecule from a simple protein mixture.

2. Materials and methods

2.1 Materials

The base matrices, Sepharose CL-6B (Cat. no. 170160-01, Lot no. 10040943), Superose 6 Prep Grade (Cat. no. 17-0489-01, Lot. no. 10037732) and Superose 12 Prep Grade (Cat. no.17-0536-01, Lot. no. 10057699) were all supplied by GE Healthcare Life Sciences (Little Chalfont, Bucks, UK). The chemicals, *N*-isopropylacrylamide (Cat. no. 415324, 97%; NIPAAm), *N*-*tert*-butylacrylamide (Cat. no. 411779, 97%; *t*-BAAm), acrylic acid (Cat. no. 147230, anhydrous, 99%, AAc), 2-ethoxy-1-ethoxycarbonyl-1,2-dihydroquinoline (Cat. no. 149837, ≥99%; EEDQ), 4,4′-azobis(4-cyanovaleric acid) (Cat. no. 11590, ≥98%; ACV), *N,N*-dimethylformamide (Cat. no. 270547, >99.9%; DMF), *N*,*N*′-methylenebisacrylamide (Cat. No. 146072, 99%; MBAAm), epichlorohydrin (Cat. no. E1055, 99%; ECH), tetrahydrofuran (Cat. no. 34865, >99%; THF), diethyl ether (Cat. no. 309966, >99.9%), sodium borohydride (Cat. no. 71321, >99%) and sodium hydroxide (Cat. no. S5881, anhydrous, >98%) were

obtained from Sigma-Aldrich Company Ltd (Poole, Dorset, UK). Absolute ethanol (Cat. no. E/0650DF/17, 99.8+%) and ammonia solution (Cat. no. A/3280/PB15, AR grade, 0.88 S.G., 35%) were acquired from Fisher Scientific UK Ltd (Loughborough, Leics, UK), and bottled oxygen-free nitrogen gas was supplied by the British Oxygen Co Ltd (Windlesham, Surrey, UK). Bovine whey lactoferrin (MLF-1, Lot. No. 12011506, ~96%) was a gift from Milei GmbH (Leutkirch, Germany), and bovine serum albumin (BSA, Cat. No. A7906, lyophilized powder, ≥98% by agarose gel electrophoresis) and 'Blue Dextran MW 2,000,000' (Cat. No. D-5751) were purchased from Sigma-Aldrich. Di-sodium hydrogen phosphate (Cat. no. 4984.1, dihydrate, ≥99.5%) was from Carl Roth GmbH + Co. KG (Karlsruhe, Germany). Disodium hydrogen phosphate (dihydrate, ≥99.5%) and sodium chloride (ACS reagent, ≥99.5%) were supplied by Carl Roth or Sigma-Aldrich, and citric acid monohydrate (≥99%) and Coomassie Brilliant Blue R250 (C.I. 42660) were from Merck Millipore (Darmstadt, Germany). Pre-cast 15% mini-PROTEAN® TGX™ gels and Precision Plus Protein™ All Blue Standards were supplied by Bio-Rad Laboratories Inc. (Hercules, CA, USA). All other chemicals not stated above were from Sigma-Aldrich or Merck Millipore. The water used in all experiments was deionized and purified using a Milli-Q Ultrapure system (Merck Millipore, Darmstadt, Germany.

2.2 Preparation of the thermoCEX media used in this work

For detailed descriptions of the procedures involved in the four step conversion of underivatized beaded agarose chromatography supports into thermoCEX media, the reader is referred to our previous study [23]. Exactly the same methods were applied here to three different beaded agarose starting materials (i.e. Sepharose CL-6B, Superose 6 Prep Grade and Superose 12 Prep Grade; see Tables 1 and 2). The first three steps of the conversion, i.e. epoxy activation, amine capping and immobilization of the ACV radical initiator were identically performed, but in the fourth and final 'graft from' polymerization step the initial

AAc monomer concentration entering reactions with ACV anchored supports was systematically varied between 25 and 150 mM (equivalent to 2.5 to 13.5% of the total monomer concentration), whilst maintaining fixed concentrations of all other monomers, i.e. 900 mM NIPAAm, 50 mM tBAAm, and 10 mM of the cross-linking monomer, MBAAm. For point of comparison, the AAc concentration used in our previous study [23] was 50 mM (corresponding to ~5% of the total monomer composition).

2.3 Batch adsorption experiments with LF

In batch binding tests, portions of settled thermoCEX matrices (0.1 mL), previously equilibrated with 10 mM sodium phosphate buffer, pH 6.5, were mixed with 0.5 mL aliquots of varying initial LF concentration (c_0 = 1 – 15 mg/mL made up in the same buffer) and incubated at 10, 20, 35 or 50 °C with shaking at 100 rpm in a Thermomixer Comfort shaker (Eppendorf, Hamburg, Germany) for 1 h. After an additional 0.5 h at the selected temperature without shaking, the supernatants were carefully removed and analyzed for residual protein content (see 2.4 Analysis). The equilibrium loadings on supports (q^*) were computed from the differences in initial (c_0) and equilibrium (c^*) bulk phase protein concentrations, and the resulting q^* vs. c^* data were subsequently fitted to the simple Langmuir model (Eq. (1))

$$q^* = q_{\max} \frac{c^*}{K_d + c^*} \qquad (1)$$

where q_{max} and K_d are respectively, the maximum protein binding capacity of the support and the dissociation constant. Data fitting was performed by SigmaPlot® software version 11 (Systat Software Inc., San Jose, CA, USA) using the least squares method.

2.3. TCZR chromatography experiments

All chromatographic experiments were conducted using Travelling Cooling Zone Reactors (TCZRs) connected to ÄKTA Purifier UPC 10 or Explorer 100 Air chromatography workstations (GE Healthcare, Uppsala, Sweden) For detailed descriptions of the TCZR arrangement, the reader is referred to our recent study [23]. A brief, but necessary description of the workings of the system is given here. The TCZR set-up features four components, i.e. (i) a temperature controlled box housing, (ii) the thermoresponsive stationary phase contained in (iii) a stainless steel walled (1 mm thick) fixed-bed column (length = 10 cm; internal diameter = 6 mm; volume = 2.83 mL), and (iv) a movable assembly of copper blocks and Peltier elements surrounding a small discrete zone of the column. The whole cooling unit can be moved up or down the column's length via a ball bearing guided linear motorized axis, and by adjusting the Peltier elements, the centre of the assembly can be cooled down by >20 °C. In all of the work described here, the constant surrounding temperature was 35 °C, and the velocity of the TCZ assembly (v_c) was the lowest attainable in the system (0.1 mm/s), generating a maximum temperature difference of 22.6 °C corresponding to a minimum temperature in the centre of the column of 12.4 °C extending across 2 cm of column length.

2.3.2 Batch mode TCZR chromatography of LF

LF (c_f = 2 mg/mL) in an equilibration buffer of 10 mM sodium phosphate, pH 6.5 was continuously applied to beds of thermoCEX media (packing factor = 1.2) until almost complete breakthrough had been achieved in each case (i.e. c/c_f approaching 1). At this point the LF saturated columns were then washed with 5 CVs of equilibration buffer, before moving the TCZ assembly multiple times (8 times in the case of thermoCEX-CL6B and thermoCEX-S6pg, and 12 times for thermoCEX-S12pg) along the full separation column's length at its minimum velocity of 0.1 mm/s, generating a minimum temperature in the centre of the column of 12.4 °C [23]. On completion of TCZ's last movement residually bound LF

was dislodged from the columns using a 1 M NaCl step gradient. Constant mobile phase velocities of 30 mL/h for the small particle sized Superose based thermoCEX media, or 60 mL/h for the larger Sepharose CL-6B derived thermoCEX adsorbent, were employed, giving rise to interstitial velocities for the packed columns of thermoCEX-S6pg, thermoCEX-S12pg and thermoCEX-CL6B of 0.70 mm/s, 0.84 mm/s and 1.89 mm/s respectively. The percentages of LF in each of collected peaks were calculated by dividing the LF mass eluted in each by the total mass of LF recovered in all of the elution peaks.

2.3.3 Continuous TCZR chromatography

In continuous chromatography experiments, feeds of LF (c_f = 0.5 or 1 mg/mL) or 'LF + BSA (1 mg/mL of each) in 10 mM sodium phosphate equilibration buffer were continuously fed at a temperature of 35 °C, and interstitial velocity of 0.74 mm/s on to a column filled with thermoCEX-S6pg. During the first 2 h of operation the TCZ remained in its parking position above the separation column, by which point the protein loading front had approached ~75% of the column's length. At this stage slow constant movement of the TCZ along the column was initiated resulting in the first elution peak. At the applied velocity (v_c = 0.1 mm/s) the TCZ travelled down the column at less than a seventh the rate of the interstitial mobile phase velocity. On reaching the base of the column, some ~20 minutes later, the elution peak left the column, and the TCZ was once again moved, at high speed, to its parking position above the column. Seven further movements of the TCZ along the column's length were conducted in each experiment at regular 80 minute intervals, i.e. after 200, 280, 360 440, 520, 600 and 680 minutes had elapsed. During the continuous application of the TCZR system, desorbed proteins were fractionated after every movement of the TCZ. The fractionation started when the UV adsorption at 280 nm in the effluent showed values above 100 mAu. The protein peaks were collected and the protein concentration was determined. Residual bound protein finally was eluted by an increase to 1 M of sodium chloride in the mobile phase. The

concentration factor ($CF_{Peak,i}$) of every single protein peak *i* was determined by dividing the protein peak concentration by the feed concentration (Eq. (2)):

$$CF_{Peak,i} = \frac{c_{Peak,i}}{c_f} \quad (2)$$

where $c_{Peak,i}$ is the peak concentration of the respective fractionated protein peak. An averaged concentration factor (*CF*) was determined by calculating the average of the peak concentration factors when a steady-state was reached (Eq. (3)):

$$CF = \frac{\sum CF_{Peak,i}}{j} \quad (3)$$

where *j* is the number of fractionated protein peaks in a steady-state. By multiplying the protein concentration of the fractions and the fraction volume, the eluted protein mass could be calculated.

2.4 Analysis

The battery of methods employed to characterize the various thermoCEX adsorbents prepared in this work, including all intermediates in their manufacture, are summarized briefly below and described in detail elsewhere [23].

Reactive epoxide contents introduced by activation with epichlorohydrin were determined as described by Sundberg and Porath [25].

For qualitative FT-IR analysis of solid supports, oven dried samples (~3 mg) were mixed with potassium bromide (300 mg), ground down to a fine powder and hydraulically pressed (15 tonne) into tablet form. Each tablet was subjected to 64 scans (averaged at a resolution of 2 cm^{-1}) in a Nicolet 380 FT-IR (Thermo Fisher Scientific, Waltham, MA, USA) in direct beam mode. Quantitative estimation of 'NIPAAm + tBAAm' consumption by supports during grafting reactions, by monitoring changes in area of the characteristic peak for N-H bending (1575 –1500 cm^{-1}), was performed on liquid samples (150 μL) applied directly to the surface of the Nicolet 30 FT-IR's Smart 53 Orbit diamond accessory. The samples were scanned 64 times at a resolution of 2 cm^{-1} in attenuated total reflectance mode (ATR FT-IR).

Gravimetric analyses was used to determine the immobilized ACV and copolymer contents on solid supports and also of dried residues recovered from liquid samples, to allow determination of free ungrafted copolymer content and unreacted monomers remaining in solution post-grafting. Free copolymers were separated from unreacted monomers by rotary evaporating to dryness, resuspending in tetrahydrofuran, precipitating with diethyl ether and oven drying, and unreacted monomers remaining in the supernatants were recovered by rotary evaporating to dryness.

The relative amounts of NIPAAm and tBAAm in ungrafted copolymers were obtained by proton NMR spectroscopic analysis of $CDCl_3$ dissolved samples using a Bruker AV400 NMR Spectrometer (Bruker-BioSpin Corporation, Billerica, MA, USA). 'NIPAAm:tBAAm' ratios (Tables 1 & 2) were computed from characteristic chemical shifts in ^1H NMR spectra at 1.15 ppm and 1.34 ppm for two strong methyl proton peaks arising from the NIPAAm and tBAAm side chains respectively [22,23].

Full temperature dependent 'coil–globule' transition profiles and lower critical solution temperature (LCST) values for ungrafted copolymers were obtained by monitoring the optical transmittance (at λ = 500 nm) of test solutions (0.5% w/v copolymer in 10 mM sodium phosphate, pH 6.5) in a Cecil CE7500 UV/visible dual beam spectrometer equipped with a water thermostatted cuvette holder.

H^+ exchange capacities of supports were determined by titration using GE Healthcare's method for determination of the ionic capacity of CM Sepharose media (No. 30407). The void volumes of packed beds of thermoCEX media were determined by SEC of Blue Dextran (50 µL, 1 mg/mL) under non binding conditions, using an equilibrating and mobile phase of 50 mM Tris-HCl, pH 7.5 supplemented with 100 mM KCl.

The protein content in samples was spectrophotometrically assayed at a wavelength of 280 nm either off-line during batch binding experiments using a NanoDrop® ND-1000 Spectrophotometer (Thermo Fisher Scientific, Waltham, MA, USA) or quartz cuvettes in a Lambda 20 UV-vis spectrophotometer (PerkinElmer Analytical Instruments, Shelton, CT, USA), or on-line during chromatographic investigations using ÄKTA chromatography workstations operated under Unicorn™ software (GE Healthcare, Uppsala, Sweden).

The composition of fractions generated during continuous TCZR chromatographic separation of LF and BSA was examined by reducing SDS-PAGE [26] in 15% (w/v) pre-cast polyacrylamide gels in a Mini-Protean® Tetracell electrophoresis system (Bio-Rad Laboratories, Hercules, CA, USA). After electrophoresis, gels were stained with 0.1% (w/v) Coomassie Brilliant Blue R250, dissolved in 40% (v/v) ethanol and 10% (v/v) acetic acid) for 1 h at room temperature, and were subsequently destained at the same temperature in a solution composed of 7.5% (v/v) acetic acid and 10% (v/v) ethanol. The LF and BSA contents

were determined by densitometric analysis of scanned TIFF images of appropriately loaded Coomassie Blue stained gels following electrophoresis. The images were captured with an HP ScanJet C7716A flat bed scanner (Hewlett-Packard Company, Palo Alto, CA, USA) at a resolution of 2400 dpi, and analyzed using ImageJ software [27].

3. Results and discussion

3.1 Concept of single-column continuous chromatography

Schematic concentration and loading profiles within the TCZR fitted column are illustrated in Fig. 2 for the various operation phases. These are characterized by different positions of the TCZ relative to the column. The profiles at three different positions of the TCZ are shown, i.e.: (i) outside the column (Fig. 2a); and after travelling (ii) a quarter (Fig. 2b) and (iii) three-quarters (Fig. 2c) of the separation column's length. When the TCZ is parked 'outside' (Fig 2a), the whole column is operated at an increased temperature (T_B). Protein is continuously loaded and binds to the adsorbent. In keeping with the binding strength of the protein to the support at T_B, sharp concentration and loading fronts of the protein propagate through the system at a constant velocity, v_{pf} (Eq. (4)):

$$v_{pf} \cong \frac{u_i}{1+\frac{1-\varepsilon_b}{\varepsilon_b}\frac{\partial q}{\partial c}} \qquad (4)$$

Here, v_{pf} is a function of the slope of the isotherm, $\frac{\partial q}{\partial c}$, the interstitial fluid velocity, u_i, and the phase ratio between the solid and liquid phases expressed by the bed voidage, ε_b, of the column packing.

When the TCZ starts to move along the column, previously bound protein desorbs at the front of the zone, resulting in a strong increase in mobile phase protein concentration (Fig. 2b, lower trace). Because the TCZ's velocity (v_c) is slower than that of the mobile phase (i.e. $v_c < u_i$), the flow transports the desorbed protein further along the column into the adjacent region, which is still at the elevated temperature, T_B. At T_B, this increased protein concentration leads to a corresponding rise in the local protein loading at this point within the column. When, sometime later, the constantly moving TCZ reaches this 'protein-laden' part of the column, its action desorbs the bound protein, resulting in an even larger surge in mobile phase protein concentration. In essence, what results within the column, provided that mass transfer limitations are small, are sharp concentration and loading waves formed in front of the moving TCZ. The concentration of adsorbing species will be much higher than that in the feed, and protein loading closely approaches the maximum capacity of the adsorbent. With progressive movement of the TCZ along the column more and more protein is desorbed at its front, to continuously supply the immediately flanking high temperature (T_B) region ('over-travelled' column section) with an increasing protein challenge (Fig. 2c. lower trace). Given that the adsorbent's protein binding capacity cannot be exceeded (Fig. 2c, upper trace) the protein concentration wave broadens (Fig. 2c, lower trace).

Closer scrutiny of the plots in Fig. 2 reveals further noteworthy features of the TCZR principle highlighted as follows:

1. When the rate of progress of the feed concentration front along the column is slower than that of the TCZ, an increasingly wide region of low protein loading and concentration forms in the TCZ's wake (compare Figs 2b & 2c). The extent of reduction in protein loading and concentration, and therefore in effect the operational working capacity of the TCZR, are determined by the TCZ's efficiency in eluting the adsorbed protein.

2. When the protein wave cresting the TCZ reaches the column outlet, protein elutes in high concentration. In the meantime, the protein feed is continuously applied at the other end of the column (inlet), protein loading of the front section of the column attains equilibrium with the feed, and once this loaded section reaches ~70% of the column length, another movement of the TCZ is initiated, giving rise to a second elution peak, and so on and so forth.

3. Thus, by careful selection of both the velocity of the TCZ and the timing between successive movements of the device, a quasi-stationary state operation should be attained, where similar concentration and protein loading profiles are generated before every movement of the TCZ. This confers unique capabilities on the TCZR system, namely the possibility of continuously loading protein at one end of column whilst simultaneously desorbing previously bound protein from the other, in a single-column installation without need of additional steps of regeneration and/or equilibration.

3.2 Manufacture and characterization of thermoresponsive CEX adsorbents

Three types of beaded cross-linked agarose matrices (Sepharose CL-6B, Superose 6 Prep Grade and Superose 12 Prep Grade) differing in particle diameter, agarose content and pore size (see Tables 1 and 2) were fashioned into thermoCEX adsorbents in four successive steps, i.e. epoxide activation, amine capping, ACV initiator immobilization and graft-from polymerization using improved protocols detailed previously [23]. The initial composition of monomers entering the final copolymer grafting step was systematically varied to create families of thermoCEX materials with different balances of thermoresponsive, hydrophobic and charged building blocks in the copolymers anchored to their exteriors and lining their pores. The resulting thermoCEX adsorbents and intermediates in their manufacture (both supports and reaction liquors) underwent rigorous qualitative and quantitative phyiscochemical analysis prior to use.

FTIR spectra obtained during the stepwise conversion of Superose 6 Prep Grade into the thermoCEX-S6pg adsorbent family are shown in Fig. 3. Identical sets of spectra were obtained with Superose 12 Prep Grade and Sepharose CL-6B subjected to the same procedures. During the various steps, the expected peaks previously assigned in converting Sepharose CL-6B into a thermoresponsive cation exchanger [23], were also observed during the manufacture of the Superose based thermoCEX media in this work. Of special note are: (i) the growth in peak heights between 1474 and 1378 cm^{-1} in the spectrum of epoxy-activated S6pg due to increased alkyl group content, consistent with incorporation of glycidyl moieties into S6pg; (ii) sharpening and growth of the signal at 1378 cm^{-1} following amination of epoxy-activated S6pg, likely arising from diminished flexibility, and therefore reduced variance in the vibrational frequency of the CH_2 groups in the backbone; (iii) the appearance of two new peaks in the FTIR spectrum of ACV immobilized S6pg (1736 cm^{-1} for carboxylic acid C=O stretching, and 1552 cm^{-1} for azo N=N stretching and/or amide N-H bending); the growth of (iv) amide N–H bending (1570 cm^{-1}) and amide C=O stretching (1670 cm^{-1}) contributions from incorporated NIPAAm, tBAAm and MBAAm units, and (v) of carboxylic acid C=O stretching (1736 cm^{-1}), arising from the presence of AAc in the grafted copolymer on the thermoCEX supports; and finally that (vi) despite marked differences in the compositions of grafted copolymers on thermoCEX supports B1-B4 (see Table 2), their FTIR spectra appear identical.

Analysis of the immobilized copolymer compositions of Sepharose CL-6B and Superose based thermoCEX (Tables 1 and 2 respectively) illustrates marked differences. Under identical reaction conditions, unique monomer consumption preferences appear to be displayed by the different ACV-coupled supports. Compare supports ‘A2’, ‘B2’ and ‘C1’ for example. When normalized against the initial monomer composition entering polymerization reactions with ACV immobilized supports, ACV-immobilized Sepharose CL-6B consumed

tBAAm and AAc roughly equally (32.5% *cf.* 30.4%), and ~2.4 times more readily than NIPAAm (13.2%); by contrast, ACV-coupled S6pg consumed tBAAm (33.5%) in >1.8 fold preference to both AAc (19.0%) and NIPAAm (18.7%), whereas ACV-linked S12pg consumed tBAAm (39.2%) ~1.5 and ~2.2 fold more readily than AAc (25.4%) and NIPAAm (17.6%) respectively. Thus, despite the higher initial epoxide density (878 μmol/g) driving increased ACV immobilization (568 μmol/g) and ~1.4 fold higher mass of grafted copolymer, the ionic capacity of the thermoCEX-S6pg was 38% lower than that on thermoCEX-CL6B (i.e. 293 *cf.* 469 μmol/g dried support), whereas its NIPAAm and tBAAm contents had both increased (by 42% and 3% respectively). We observed this phenomenon previously during fabrication of thermoCEX adsorbents fashioned from ostensibly very similar cross-linked 6% agarose media, and suggested that differences were likely linked to the epoxide densities introduced in the first synthetic step, rather than to subtle chemical disparities between the two base matrices [23]. Based on findings in this study with 15 support materials, i.e. 9 finished thermoCEX and 6 intermediates in their manufacture (Tables 1 & 2), we no longer believe this to be the case. Though sharing agarose backbones and being subjected to identical polymer modification reactions, it appears here that differences in proprietary modification (principally cross linking) of the base matrix starting materials [29-33] influence the initial epoxy activation level, subsequent immobilized initiator density, loading and composition of grafted copolymer of the finished thermoCEX adsorbents.

Sepharose CL-6B is prepared by first reacting Sepharose 6B with 2,3-dibromopropanol under strongly alkaline conditions and then desulphating post cross-linking, by reducing alkaline hydrolysis, to give a cross-linked matrix with high hydrophilicity and very low content of ionizable groups [30,33]. In the manufacture of Superose media, cross-linking to confer rigidity occurs in two stages, i.e. initial priming reaction with a cocktail of long-chain bi- and poly- functional epoxides in organic solvent, followed by cross-linking via short-chain bi-

functional cross-linkers conducted in aqueous solvent [30,32]. Superose media are thus less hydrophilic than Sepharose CL supports, and it is this fundamental difference that likely: (i) contributes to the 30 – 50% greater number of immobilized oxiranes introduced into Superose matrices (Table 2, 878 μmol/g for S6pg, 1018 μmol/g for S12pg) by epichlorohydrin activation (step 1) under identical conditions *cf.* Sepharose CL-6B (Table 1, 662 μmol/g); leads in turn (ii) both to higher immobilized ACV contents (568 – 611 μmol/g for S6pg, 878 μmol/g for S12pg *cf.* 380 μmol/g for Sepharose CL-6B) and elevated grafted polymer yields (6005 ± 68 μmol/g for ThermoCEX-Superose adsorbents *cf.* 4675 ± 97 μmol/g for ThermoCEX-CL6B); and (iii) significantly higher incorporation of the charged AAc monomer into the grafted copolymers on ThermoCEX-CL6B *cf.* ThermoCEX adsorbents fashioned from Superose media across all AAc input concentrations during grafting (see Tables 1 and 2).

The temperature dependent phase transition behaviour of ungrafted free copolymer solutions emanating from various grafting reactions with ACV-immobilized Sepharose CL-6B and Superose Prep Grade are compared in Fig. 4. Figures 4a and 4b display the raw transmittance vs. temperature profiles, and Fig. 4c examines the wider impact of NIPAAm replacement on the LCST and full transition temperature ranges of the copolymers.

In accord with literature reports [12-14], the LCST at 50% optical transmittance ($T_{50\%}$) for the 'smart' homopolymer pNIPAAm was 32.3 °C and sharp transition from fully extended 'hydrophilic coil' ($T_{90\%}$) to fully collapsed 'hydrophobic globule' ($T_{0.4\%}$) occurred between 31 and 35 °C (dashed line traces in Figs 4 a-c). Copolymerizing NIPAAm with more hydrophobic monomers leads to a reduction in the LCST [34,35], whereas incorporation of more hydrophilic species increases it [34]. Here, simultaneous low level substitution of AAc

and tBAAm into pNIPAAm's backbone ('A1', 'B1' & 'C1') at the expense of 12.1 to 16.9% of its NIPAAm content (Tables 1 & 2), had the effect of lowering the LCST (by 1.4 °C for 'A1', 2.3 °C for 'B1', 1.5 °C for 'B2' and 0.9 °C for 'C1') and broadening the transition temperature range in both directions (i.e. 28.3 to 36.7 °C for 'A1', 26.5 to 34.8 °C for 'B1', 26.5 to 37.7 °C for 'B2', and 28.5 to 36.8 °C for 'C1'). With mounting NIPAAm replacement ('A3', 'A4', 'B3', 'B4'), smart thermoresponsive behaviour became increasingly compromised. For example, the LCST for the '67.3:15.8:16.9' copolymer (Fig. 4d, 'A4') reached 36.6 °C and temperature range over which full 'coil – globule' transition range extended >25 °C, i.e. from 20.5 to 46 °C.

3.3 Temperature dependent adsorption of LF on thermoCEX adsorbents

The optimum condition for an effective thermoresponsive adsorbent is one where the binding of a given target is strongly temperature dependent; in the ideal case being effectively switched 'on' (powerful adsorption) and 'off' (no adsorption) by a small change in bulk phase temperature across the LCST of the thermoresponsive copolymer. In practice this has not been achieved, i.e. the sharp 'coil – globule' transitions observed in free solution are not mirrored by protein binding vs. temperature plots [22,23]. The collapse and extension of surface-anchored thermoresponsive copolymer chains is considerably more constrained [36] and complex [23,36,37] than that of the free untethered species. As a consequence, changes to the binding interface in response to a thermal trigger are gradual in nature.

The effect of temperature on the maximum LF adsorption capacity (q_{max}) for all nine thermoCEX supports is illustrated in Fig. 5. In all cases, q_{max} rose linearly with increase in temperature over the examined range (10 – 50 °C), as the tethered copolymer networks gradually transitioned from predominantly hydrophilic and fully extended low charge density states (Fig. 1, bottom right) to increasingly flattened, hydrophobic and highly charged ones

(Fig. 1, top right), as the distance between neighboring charged AAc units within the collapsed copolymer decreased and previously shielded/buried negative charges became exposed [22]. However, the degree of thermoresponsiveness exhibited varied significantly between and within each thermoCEX family, and a clear trend emerged. For the least substituted supports in the Sepharose CL-6B and Superose 6pg thermoCEX families, i.e. 'A1' (Fig. 5a, Table 1) and 'B1' (Fig. 5b, Table 2), LF binding capacity was strongly temperature dependent ('$q_{max,\,50°C}$ / $q_{max,\,10°C}$' ratios of 2.2 for 'A1' & 3.3 for 'B1'), but low ($q_{max,50°C}$ values of <22 mg/mL for 'B1' and <27 mg/mL for 'A1'). With increasing NIPAAm replacement by hydrophobic tBAAm and negatively charged AAc monomers (➞'A2'➞'A3'➞'A4', Fig. 5a; ➞'B2'➞'B3'➞'B4'; Fig. 5b), LF binding increased dramatically ($q_{max,\,50°C}$ rising to ~52 mg/mL for 'B4' and ~83 mg/mL for 'A4'), but became increasingly temperature independent ('$q_{max,\,50°C}$ / $q_{max,\,10°C}$' ratios of 1.06 for A4 & 1.1 for 'B4'), as the ability of the tethered copolymers to transition between extended and collapsed states was lost. ThermoCEX supports with moderate levels of NIPAAm replacement, i.e. 'A2', 'B2' & 'C1', displayed the best combination of thermoresponsiveness and LF binding capacity (i.e. reasonable $q_{max,\,50°C}$ and low $q_{max,10°C}$ values), and were therefore selected for further study.

Fig. 6 shows adsorption isotherms obtained for the binding of LF to these at different temperatures, and Table 3 presents the fitted Langmuir parameters. At the lowest temperature of 10 °C, the binding of LF to all three thermoCEX adsorbents is rather weak (K_d values between 0.82 and 4.8 mg/mL) and of low capacity (q_{max} values <17 mg/mL), but as the temperature is gradually stepped up, the tightness and capacity of LF sorption rise strongly. At the highest temperature of 50 °C, the paired values for q_{max} and tightness of binding (initial slope, q_{max}/K_d) are 55.9 mg and 631 for support 'A2', 28.6 mg/mL and 168 for 'B2', and 44.7 mg/mL and 213 for support 'C1' (Table 3). An identical pattern of behaviour in response to temperature (between 20 and 50 °C) was noted previously by Maharjan et al. [22] for a

thermoCEX support fashioned out of Sepharose 6 FF. The ranking of static LF binding performance of this family of thermoCEX supports of 'Sepharose CL-6B > Superose 12 Prep Grade > Superose 6 Prep Grade > Sepharose 6 FF' (initial slope values at 50 °C of 610, 213, 168 and 120 respectively) is not correlated with mass of copolymer attached (respectively 4177, 5495, 5733, 2060 μmol/g dried support), nor the tBAAm content (respectively 501, 604, 516, 165 μmol/g dried support), but rather with the support's intrinsic ionic capacity (i.e. 469 μmol > 391 μmol > 293 μmol > 154 μmol H^+/g dried support).

Figure 7 compares chromatographic profiles arising from batch TCZR chromatography of LF on fixed beds of three thermoCEX manufactured under identical conditions from cross-linked agarose base matrices differing in particle diameter and pore size (see Tables 1 & 2), i.e. thermoCEX-CL6B 'A2' (Fig. 7a), thermoCEX-S6pg 'B2' (Fig. 7b) and thermoCEX-S12pg 'C1' (Fig. 7c). A striking similarity is instantly evident, namely that every movement of the TCZ results in a sharp LF elution peak. Of greater importance, however, are the differences. Following 8 movements of the TCZ along beds of the thermoCEX-CL6B 'A2' (Fig. 7a) and thermoCEX-S6pg 'B2' (Fig. 7b), the percentages of eluted LF recovered in peaks '*a*' to '*h*' combined were practically the same, i.e. 64.6% of that initially bound for thermoCEX-CL6B 'A2' *cf.* 67.1% for thermoCEX-S6pg 'B2'. But whereas just over half (54.4%) of the thermally eluted LF from all 8 peaks ('*a – h'*) was recovered by the first movement of the TCZ (peak '*a*') along the thermoCEX-CL6B 'A2' column (Fig. 7a), peak '*a*' accounted for more three-quarters (76.6%) of the combined thermally eluted LF (*a – h* inclusive) from thermoCEX-S6pg 'B2' (Fig. 7b). Twelve movements of the TCZ were employed during TCZR chromatography on thermoCEX-S12pg 'C1'. In this case, eluted LF recovered in peaks '*a – l'* was just 58.3%, and the first movement of the TCZ accounted for only 17.5% of combined thermally eluted LF ('*a – l*').

Achieving significantly higher LF desorption with a single movement of the TCZ, i.e. approaching the 100% level, would require the absence of both mass transport limitations and LF binding at the minimum column temperature of 12.4 °C. Clearly, neither condition applies. Inspection of Fig. 6 and Table 3 confirm that LF is still able to bind to the thermoCEX media at 10 °C albeit weakly, thus at 12.4 °C in the TCZR system some LF will inevitably remain bound. Further, evidence of significant limitations on mass transport during TCZR mediated elution (though noticeably less marked for thermoCEX-S6pg 'B2') is provided by the observation that LF elution continued up to and including the last TCZ movement for all three matrices (Fig. 7). Because the total amounts of LF eluted on approaching equilibrium (after 8 movements of the TCZ) were essentially the same for thermoCEX-CL6B 'A2' and thermoCEX-S6pg 'B2', the lower LF binding strength of thermoCEX-S6pg 'B2' cannot adequately explain its improved LF recovery following the first TCZ movement (peak '*a*' in Figs 7 a & b). Instead, differences in particle size and pore diameter (highlighted in Tables 1 & 2) manifested in form of pore diffusion limitation, likely account for the significant disparity in % LF desorption observed following the first TCZ movement along packed beds of the three different thermoCEX media, i.e. 76.6% for thermoCEX-S6pg 'B2' *cf.* 55.4% for thermoCEX-CL6B 'A2' *cf.* 17.5% for thermoCEX-S12pg 'C1'.

Consider the case of a target protein adsorbed close to the centre of a thermoCEX support particle. If such a species is to be desorbed by the temperature change effected by the TCZ, it must diffuse out of the support particle's pores and into the mobile phase to be eluted from the column. However, should the time required for this diffusion process be greater than the TCZ's contact time with the region of the column where the support resides, the target protein will re-adsorb en route and hence will not contribute to the elution peak. The advantage of smaller adsorbent particle diameters and adequately large pores for TCZR application with

583 protein adsorbates is therefore clear. Smaller particles dictate shorter diffusion paths, while
584 large pores provide less of an impediment to mass transfer of large macromolecules [38]. This
585 combination leads to reduced times for the diffusion process, culminating practically in fewer
586 numbers of movements of the TCZ to achieve a desired target desorption yield, and is
587 displayed best in this work by the Superose 6 Prep Grade based thermoCEX matrix.
588

589 **3.4 Continuous protein accumulation experiments**

590 In our first series of continuous TCZR chromatography experiments, the influence of the
591 target protein concentration (c_f) on total system performance during continuous feeding and 8
592 movements of the TCZ along the column was examined using LF as the model binding
593 component and thermoCEX-S6pg 'B2' as the column packing material. Chromatograms
594 corresponding to continuous feeding of LF at 0.5 mg/mL and 1 mg/mL are shown in Figs 8a
595 and 8b respectively. In both cases, residual bound LF not desorbed by the TCZ was eluted
596 after the last movement by raising the mobile phase's ionic strength.
597

598 Visual comparison of the 8 individual eluted peaks (a – g) within each chromatogram
599 suggests a certain time is required before the profiles and peak areas become uniform (i.e. 4
600 movements at c_f = 0.5 mg/mL and 3 movements at c_f = 1 mg/mL), and the quantitative
601 analysis in Table 4 confirms this. Quasi-stationary states are effectively reached from peaks
602 '*d*' (c_f = 0.5 mg/mL) and '*c*' (c_f =1 mg/mL) onwards, where the mass of LF eluted in each
603 peak remains essentially constant (i.e. 14.2 ± 2.1 mg and 30.7 ± 1.3 mg for the low and high
604 LF feed concentrations respectively) and small traces of LF are lost in the flowthrough
605 between successive individual elution peaks (i.e. averages of 1.5 and 2.6 mg for low and high
606 LF feed conditions respectively). The observation that steady state was reached later, when
607 feeding the lower strength LF feed, merits explanation. Attaining a quasi-stationary condition
608 is only possible after the TCZ has completed its transit and the protein loading across the full

column length approaches equilibrium. Under such circumstances, the amount of protein temporarily loaded at the elevated temperature T_B, (with the TCZ parked outside, Fig. 2a) will be constant. From this it follows that raising the protein concentration in the feed should speed the acquisition of a steady state.

Another important parameter influenced by the protein concentration in feed is averaged concentration factor, *CF*, (Eq. (3)) attainable during steady state operation. The *CF* reached 9.2 at c_f = 0.5 mg/mL (Fig. 8a), but dropped to 7.9 on increasing the LF concentration in the feed twofold (Fig. 8b). An explanation for the slight reduction in *CF* with increasing LF concentration can be found in the isotherm describing LF adsorption to thermoCEX-S6pg 'B2' at 35 °C (Fig. 6b); i.e. isotherm starts to become non-linear between 0.5 and 1 mg LF per mL.

3.5 Continuous separation of a binary protein mixture

The ability of TCZR to function continuously having been established (Fig. 8, Table 4), the next step was to test TCZR's feasibility to not only accumulate and concentrate a single target protein, but to continuously separate it from a protein mixture. For this we employed a simple binary protein mixture consisting 1 mg/mL LF and 1 mg/mL BSA in a 10 mM sodium phosphate pH 6.5 buffer. At this pH the binding species LF carries an overall cationic charge, whereas the BSA is negatively charged. The experiment was conducted in a similar manner to the LF accumulation study reported above (Section 3.4, Fig. 8), and Fig. 9 shows the chromatogram obtained. Shortly after applying the protein mix to the column, the UV signal stepped steeply to ~350 mAU where it remained (first flowthrough pooled 'a') until directly after the first of 8 individual movements of the TCZ (highlighted by shaded gray bars). Each TCZ movement led immediately to a sharp (>2750 mAU) symmetrical elution peak, and the UV signal of the flowthrough between each temperature mediated elution peak rapidly

returned to roughly constant threshold of ~500 mAU. Following the 8th TCZ motion, residually bound protein was desorbed from the column by a step change in ionic strength (S).

SDS-PAGE analysis of the feed (F), pooled flowthrough (*c*, *e*, *g*, *i*, *k*, *m*, *o* & *q*), peak (*b*, *d*, *f*, *h*, *j*, *l*, *n* & *p*) and salt-stripped (S) fractions corresponding to the chromatogram in Fig. 9 is presented in Fig. 10. Commercial BSA and LF were employed in this work, and neither protein was subjected to further purification prior to use. Thus, the binary 'LF+BSA' mixture used actually contained many additional species present in trace quantitites. Cation exchange chromatography had been employed as the main purification step for the ~96% pure LF, and all but one contaminant species observable in Fig. 10 (esp. noticeable in pool 'S') emanates from this preparation. Only two species within the BSA preparation are observed in Coomassie Blue stained electrophoretograms following SDS-PAGE, i.e. the 66.4 kDa monomer accounting for >98% of the BSA content, and a much lower intensity 130.5 kDa dimer contaminant. The intensities of the lower migrating BSA monomer and upper dimer species remain constant across all flowthrough and peak fractions indicating their continued presence in the mobile phase throughout the run. The early UV signal surge to 350 mAU in Fig. 9 (flowthrough pool '*a*') is primarily due to breakthrough of BSA (see Fig. 10, only a small percentage of the feed's LF is noted in pool '*a*'); the sharp strong peaks, on the other hand, arise from the accumulation on and subsequent temperature mediated elution of LF along with small traces of numerous contaminants of the LF preparation (Fig. 10) from the adsorbent bed. The increase in UV signal from 350 mAU for the flowthrough pool '*a*' to 500 mAU for all inter peak flowthroughs (pools *c*, *e*, *g*, *i*, *k*, *m*, *o*, & *q*) is due to LF leakage. The addition of 1 mg/mL BSA to the 1 mg/mL LF feed did not disturb the time taken to attain quasi-stationary state; in both cases this was reached from the third peak on (compare Figs 8b and 9). However, the average eluted LF mass per peak and concentration factors were significantly lower (i.e. 21.4 mg *cf.* 30.7 mg & CF = 6.3 *cf.* 7.9), and the loss of LF in the

flowthrough between successive elution peaks was much higher (12.2 *cf.* 2.6 mg). Nevertheless, the mean purity of LF in eluted peaks was ~86%.

Reasons for impaired LF recovery in the presence of BSA are presently unclear. The presence of small amounts of BSA in the NaCl stripped pool 'S' (Fig. 10) illustrates that a tiny fraction of applied BSA had been adsorbed sufficiently strongly to resist desorption by 8 movements of the TCZ. The occurrence of BSA in the strip fraction 'S' and unbound fractions (pools *a*, *c*, *e*, *g*, *i*, *k*, *m*, *o*, & *q*) raises the possiblity of two or more distinct BSA species, i.e. those that electrostatically repelled, and others that bind strongly and possibly unfold and spread on the thermoCEX matrix at 35 °C. Such a scenario could occur were the distribution of exposed hydrophobic and charged monomers within the collapsed copolymer non-uniform, such that highly hydrophobic clusters or islands are created occupying a few percent of the overall binding surface. In this instance a slight drop in the adsorbent's LF binding capacity, but not in its LF binding affinity, would be anticipated.

A more satisfactory explanation for the reduction in both LF binding strength and capacity in the presence of BSA is fouling of binding interface by the lipids it carries. Long-chain free fatty acids (FFAs) are found in many bioprocess liquors (e.g. fermentation broths), but their influence on fouling of chromatography media and membrane units has gone largely ignored owing to their low concentrations and poor solubility [39,40]. Serum albumin's principal role *in vivo* is to bind otherwise insoluble long-chain fatty acids released into the blood from adipose cells and transport them within circulating plasma, and the effectiveness with which it binds FFAs is highlighted by the fact that the solution concentration of a given long-chain FFA can be increased as much 500 fold in its presence [41]. To date, most chromatographic studies with BSA have employed commercial preparations substantially pure with respect to protein, but not free of lipids. Procedures for delipidation of serum albumin usually involve

687 extraction with organic phases at elevated temperatures or sorption of free fatty acids (FFAs)
688 onto activated charcoal at elevated temperature under acidic–neutral conditions [41,42].
689 Under the operating conditions employed here, i.e. mobile phase of pH 6.5, temperature of 35
690 °C, FFA binding to BSA is weak [42] and FFA solubility is comparatively high [40]; it is
691 conceivable that FFAs bind to and foul the copolymer binding surface, thereby reducing both
692 the adsorbent's binding affinity and occupancy for LF.
693

694 **4. Conclusions**

695 The fabrication and detailed characterisation of porous beaded thermoCEX adsorbents
696 varying in particle size, pore dimensions and grafted poly(*N*-isopropylacrylamide-*co*-*N*-tert-
697 butylacrylamide-*co*-acrylic acid) composition has been done for two main reasons, i.e. to (i)
698 challenge an earlier hypothesis [23] that intra-particle diffusion of desorbed protein out of the
699 support pores is the main parameter affecting TCZR performance; and (ii) identify an
700 effective adsorbent customized for TCZR chromatography. ThermoCEX matrices with
701 moderate levels of NIPAAm replacement (by *N*-tert-butylacrylamide and acrylic acid)
702 displayed the best combination of thermoresponsiveness and LF binding capacity. Head-to-
703 head batch TCZR chromatography tests with LF and three such materials confirmed the
704 advantage of small particles with adequately sized pores, namely faster diffusion leading to
705 fewer numbers of TCZ movement to attain a set desorption yield.
706

707 Chromatographic separations of proteins are typically performed in batch mode requiring
708 sequential steps of equilibration, loading, washing elution and regeneration. Unless fully
709 optimized, a common feature is inefficient use of the separation medium. The switch from
710 batch to continuous operation promises several advantages, key of which is more efficient
711 utilization of the bed [43]. Several continuous chromatography formats have been developed
712 and applied for the separation of biomacromolecules thus far, including Continuous Annular

Chromatography [44], Continuous Radial Flow Chromatography [43], Simulated Moving Bed in various guises [45-49], and Periodic Counter-current Chromatography [50]. The new addition described here, Continuous Travelling Cooling Zone Reactor Chromatography, employs a single column operated isocratically. The simplicity of its configuration notwithstanding, the main benefits over batchwise operation include reduced solvent and buffer component usage, time savings and increased productivity. The continuous steady state accumulation on and regular cyclic elution of the thermostable basic protein, LF, from a fixed bed of a thermoresponsive cation exchange adsorbent in the form of sharp uniformly sized peaks has been demonstrated in this work. The time required to reach quasi steady state operation and the degree of concentration attained on TCZ mediated elution appear inversely related to the concentration of LF being continuously supplied to the bed. The addition of the non-binding species, BSA, to the LF feed had unexpectedly deleterious effects on lactoferrin accumulation and recovery; the latter being tentatively attributed to fouling of the thermoCEX matrix by lipids carried into the feed by serum albumin. No evidence of temperature induced protein unfolding during TCZR chromatography was observed in the current study, but it remains a potential problem, especially for more thermolabile proteins. Non-NIPAAm based thermoresponsive polymers tuned to transition at lower temperatures should mitigate this concern [23,51].

Currently, the primary limiters on TCZR system throughput come from the necessary use of low flow rates – a direct consequence of the prevailing mass transfer limitations. In the present example the sorbate, LF, must diffuse into and back out of individual thermoCEX adsorbent beads within a period of ~3 minutes. A small particle diameter combined with sufficiently large pores is necessary in this instance (hence Superose 6 Prep Grade's superiority over Sepharose CL-6B and Superose 12 Prep Grade), and the magnitude of the interstitial fluid velocity is practically constrained to ~1 mm/s (i.e. ~10 times the TCZ's

minimum speed of 0.1 mm/s). It should be possible to overcome the above issues by using thermoresponsive adsorbents fashioned from either more pressure tolerant smaller uniformly sized support particles with similar pore dimensions, or monolithic materials [51-53]. Future work on TZCR will explore this tenet.

Acknowledgements

This work was funded by the European Framework 7 large scale integrating collaborative project 'Advanced Magnetic nano-particles Deliver Smart Processes and Products for Life' (MagPro^{2}Life, CP-IP 229335-2).

References

[1] S.C. Goheen, B.M. Gibbins, Protein losses in ion-exchange and hydrophobic interaction high-performance liquid chromatography, J. Chromatogr. A 890 (2000) 73 – 80.

[2] J.A. Asenjo, B.A. Andrews, Protein purification using chromatography: selection of type, modelling and optimization of operating conditions, J. Molec. Recognit. 22 (2009) 65 – 76.

[3] G. Guiochon, Preparative liquid chromatography, J. Chromatogr. A 965 (2002) 129 – 161.

[4] Y. Shi, R. Xiang, C. Horvath, J.A. Wilkins, The role of liquid chromatography in proteomics, J. Chromatogr. A 1053 (2004) 27 – 36.

[5] C.J. Venkatramani, Y. Zelechonok, An automated orthogonal two-dimensional liquid chromatograph, Anal. Chem. 75 (2003) 3484 – 3494.

[6] D. Haidacher, A. Vailaya, C. Horváth, Temperature effects in hydrophobic interaction chromatography, Proc. Nat. Acad. Sci. 93 (1996) 2290 – 2295.

[7] S. Hjertén, Some general aspects of hydrophobic interaction chromatography, J. Chromatogr. 87 (1973) 325 – 331.

[8] J.A. Queiroz, C.T. Tomaz, J.M.S. Cabral, Hydrophobic interaction chromatography of proteins, J. Biotechnol. 87 (2001) 143 – 159.

765 [9] R. Muca, W. Piatkowski, D. Antos, Altering efficiency of hydrophobic interaction
766 chromatography by combined salt and temperature effects, J. Chromatogr. A 1216 (2009)
767 6716-6727.
768 [10] R. Muca, W. Piatkowski, D. Antos, Effects of thermal heterogeneity in hydrophobic
769 interaction chromatography, J. Chromatogr. A 1216 (2009) 8712 – 8721.
770 [11] L. Taylor, D. Cerankowski, Preparation of films exhibiting a balanced temperature
771 dependence to permeation by aqueous solutions – a study of lower consolute behavior, J.
772 Polym. Sci., Part A: Polym. Chem. 13 (1975) 2551 – 2570.
773 [12] M. Heskins, J.E. Guillet, Solution properties of poly(N-isopropylacrylamide), J.
774 Macromolec. Sci. A 2 (1968) 1441 – 1455.
775 [13] K. Kubota, S. Fujishige, I. Ando, Single-chain transition of poly(N-isopropylacrylamide)
776 in water, J. Phys. Chem., 94 (1990) 5154 – 5158.
777 [14] H.G. Schild, Poly(N-isopropylacrylamide): Experiment, theory and application, Prog.
778 Polym. Sci. 17 (1992) 163 – 249.
779 [15] P. Maharjan, B.W. Woonton, L.E. Bennett, G.W. Smithers, K. DeSilva, M.T.W. Hearn,
780 Novel chromatographic separation – The potential of smart polymers, Innov. Food Sci.
781 Emerg. Technol. 9 (2008) 232 – 242.
782 [16] I.Y. Galaev, B. Matthiasson, 'Smart' polymers and what they could do in biotechnology
783 and medicine, Trends Biotechnol. 17 (1999) 335 – 340.
784 [17] A.S. Hoffman, P. Stayton, Bioconjugates of smart polymers and proteins: synthesis and
785 applications, Macromol. Symp. 207 (2004) 139 – 151.
786 [18] N. Matsuda, T. Shimizu, M. Yamato, T. Okano, Tissue Engineering based on cell sheet
787 technology, Adv. Mater. 19 (2007) 3089 – 3099.
788 [19] K. Hoshino, M. Taniguchi, T. Kitao, S. Morohashi, T. Sasakura, Preparation of a new
789 thermo-responsive adsorbent with maltose as a ligand and its application to affinity
790 precipitation, Biotechnol. Bioeng. 60 (1998) 568 – 579.

791 [20] H. Kanazawa, K. Yamamoto, Y. Matsushima, N. Takai, A. Kikuchi, Y. Sakurai, T.
792 Okano, Temperature-responsive chromatography using poly(N-isopropylacrylamide)-
793 modified silica, Anal. Chem. 68 (1996) 100 – 105.
794 [21] K. Yamamoto, H. Kanazawa, Y. Matsushima, T. Nobuhara, A. Kikuchi, T. Okano,
795 Chromatogr. 21 (2000) 209 – 215.
796 [22] P. Maharjan, M.T. Hearn, W.R. Jackson, K. De Silva, B.W. Woonton, Development of a
797 temperature-responsive agarose-based ion-exchange chromatographic resin, J. Chromatogr. A
798 1216 (2009) 8722 – 8729.
799 [23] T.K.H. Müller, P. Cao, S. Ewert, J. Wohlgemuth, H. Liu, T.C. Willett, E. Theodosiou,
800 O.R.T. Thomas, M. Franzreb, Integrated system for temperature-controlled fast protein liquid
801 chromatography comprising improved copolymer modified beaded agarose adsorbents and a
802 travelling cooling zone reactor arrangement, J. Chromatogr. A 1285 (2013) 97 – 109.
803 [24] N.S. Terefe, O. Glagovskaia, K. De Silva, R. Stockmann, Application of stimuli
804 responsive polymers for sustainable ion exchange chromatography, Food Bioprod. Process.
805 92 (2014) 208 –225.
806 [25] L. Sundberg. J. Porath, Preparation of adsorbents for biospecific affinity
807 chromatography: I. Attachment of group-containing ligands to insoluble polymers by means
808 of bifunctional oxiranes, J. Chromatogr. 90 (1974) 87 – 98.
809 [26] U.K. Laemmli, Cleavage of structural proteins during the assembly of the head of
810 Bacteriophage T4, Nature (London) 227 (1970) 680 – 685.
811 [27] C.A. Schneider, W.S. Rasband, K.W. Eliceiri, NIH Image to ImageJ: 25 years of image
812 analysis, Nat. Methods 9 (2012) 671 – 675.
813 [28] M.D. Oza, R. Meena, K. Prasad, P. Paul, A.K. Siddhanta, Functional modification of
814 agarose: A facile synthesis of a fluorescent agarose–guanine derivative, Carbohydr. Polym. 81
815 (2010) 878 – 884.

816 [29] J. Porath, J.-C. Janson, T Låås, Agar derivatives for chromatography, electrophoresis and
817 gel-bound enzymes, J. Chromatogr. 60 (1971) 167 – 177.
818 [30] T. Andersson, M. Carlsson, L. Hagel, P.-A. Pernemalm, J.-C. Janson, Agarose-based
819 media for high-resolution gel filtration of biopolymers, J. Chromatogr. 326 (1985) 33 – 44.
820 [31] G.E.S. Lindgren, Method of cross-linking a porous polysaccharide gel, US Patent
821 4,973,683, Publication date: 11/27/1990.
822 [32] P.A. Pernemalm, M. Carlsson, G. Lindgren, Separation material and its preparation,
823 European Patent EP 0132244, Publication date: 12/17/1986.
824 [33] M. Andersson, M. Ramberg, B.-L. Johansson, The influence of the degree of cross-
825 linking, type of ligand and support on the chemical stability of chromatography media
826 intended for protein purification, Process Biochem. 33 (1998) 47 – 55.
827 [34] A.S. Hoffman, P. Stayton, V. Bulmus, G. Chen, J. Chen, C. Cheung, A. Chilkoti, Z.
828 Ding, L. Dong, R. Fong, C.A. Lackey, C. J. Long,M. Miura, J.E. Morris, N. Murthy, Y.
829 Nabeshima, T.G. Park, O.W. Press, T. Shimoboji, S. Shoemaker, H.J. Yang, N. Monji, R.C.
830 Nowinski, C.A. Cole, J.H. Priest, J.M. Harris, K. Nakamae, T. Nishino, T. Miyata, Really
831 smart bioconjugates of smart polymers and receptor proteins, J. Biomed. Mater. Res. 52
832 (2000) 577 – 586.
833 [35] Y. Yoshimatsu, B.K. Lesel, Y. Yonamine, J.M. Beierle, Y. Hoshino, K.J. Shea,
834 Temperature-responsive “catch and release” of proteins by using multifunctional polymer-
835 based nanoparticles, Angew. Chem. Int. Ed. 51 (2012) 2405 – 2408.
836 [36] M. Andersson, S. Hietala, H. Tenhu, S.L. Maunu, Polystyrene latex particles coated with
837 crosslinked poly(N-isopropylacrylamide), Colloid Polym. Sci. 284 (2006) 1255 – 1263
838 [37] K.N. Plunkett, Z., Xi, J.S. Moore, D.E. Leckband, PNIPAM chain collapse depends on
839 the molecular weight and grafting density Langmuir 22 (2006) 4259 – 4266.

840 [38] J.F. Langford, M.R. Schure, Y. Yao, S.F. Maloney, A.M. Lenhoff, Effects of pore
841 structure and molecular size on diffusion in chromatographic adsorbents, J. Chromatogr. A
842 1126 (2006) 95 – 106.
843 [39] J. Jin, S. Chhatre, N.J. Titchener-Hooker, D.G. Bracewell, Evaluation of the impact of
844 lipid fouling during the chromatographic purification of virus-like particles from
845 *Saccharomyces cerevisiae*, J. Chem. Technol. Biotechnol. 85 (2010) 209 – 215.
846 [39] J. Brinck, A.-S. Jönsson, B. Jönsson, J. Lindau, Influence of pH on the adsorptive fouling
847 of ultrafiltration membranes by fatty acid, J. Membr. Sci. 164 (2000) 187 – 194.
848 [41] A.A. Spector, K. John, J.E. Fletcher, Binding of long-chain fatty acids to bovine serum
849 albumin, J. Lipid Res. 10 (1969) 56 – 67.
850 [42] R. Chen, Removal of fatty acids from serum albumin by charcoal treatment removal of
851 fatty acids by charcoal treatment from serum albumin, J. Biol. Chem. 242 (1967) 173 – 181.
852 [43] M.C. Lay, C.J. Fee, J.E. Swan, Continuous radial flow chromatography of proteins, Food
853 Bioprod. Process. 84 (2006) 78 – 83.
854 [44] R. Giovanni, R. Freitag, Continuous isolation of plasmid DNA by annular
855 chromatography, Biotechnol. Bioeng. 77 (2002) 445 – 454.
856 [45] J. Andersson, B. Mattiasson, Simulated moving bed technology with a simplified
857 approach for protein purification: Separation of lactoperoxidase and lactoferrin from whey
858 protein concentrate, J. Chromatogr. A 1107 (2006) 88 – 95.
859 [46] B.J. Park, C.H. Lee, S. Mun, Y.M. Koo, Novel application of simulated moving bed
860 chromatography to protein refolding, Process Biochem. 41 (2006) 1072 – 1082.
861 [47] S. Palani, L. Gueorguieva, U. Rinas, A. Seidel-Morgenstern, G. Jayaraman, Recombinant
862 protein purification using gradient-assisted simulated moving bed hydrophobic interaction
863 chromatography. Part I: Selection of chromatographic system and estimation of adsorption
864 isotherms, J. Chromatogr. A 1218 (2011) 6396 – 6401.

865 [48] M. Bisschops, BioSMB™ Technology: Continuous Countercurrent Chromatography
866 Enabling a Fully Disposable Process, in: G. Subramanian (Ed.), Biopharmaceutical
867 Production Technology, Volume 1 & Volume 2Wiley-VCH Verlag GmbH & Co. KGaA,
868 Weinheim, Germany, 2012, pp. 769 – 791.
869 [49] M. Angarita, T. Mueller-Spaeth, D. Baur, R. Lievrouw, G. Lissens, M. Morbidelli, Twin-
870 column CaptureSMB: A novel cyclic process for protein A affinity chromatography, J.
871 Chromatogr. A 1389 (2015) 85 – 95.
872 [50] R. Godawat, K. Brower, S. Jain, K. Konstantinov, F. Riske, V. Warikoo, Periodic
873 counter-current chromatography – design and operational considerations for integrated and
874 continuous purification of proteins, Biotechnol. J. 7 (2012) 1496 – 1508.
875 [51] N. Li, L. Qi, Y. Shen, Y. Li, Y. Chen, Thermoresponsive oligo(ethylene glycol)-based
876 polymer brushes on polymer monoliths for all-aqueous chromatography, ACS Appl. Mater.
877 Interfaces, 5 (2013) 12441 – 12448.
878 [52] E.C. Peters, F. Svec, J.M.J. Frechet, Thermally responsive rigid polymer monoliths, Adv.
879 Mater. 9 (1997) 630 – 632.
880 [53] K. Nagase, J. Kobayashi, A. Kikuchi, Y. Akiyama, H. Kanazawa, T. Okano, Thermally
881 modulated cationic copolymer brush on monolithic silica rods for high-speed separation of
882 acidic biomolecules, ACS Appl. Mater. Interfaces 5 (2013) 1442 – 1452.
883

883 **Figure legends**

884

885 **Fig. 1.** Schematic illustration of the TCZR principle. A stainless steel column filled with
886 thermoresponsive copolymer modified chromatographic media is contained in a temperature-
887 controlled environment at a value above the copolymer's LCST. At this temperature
888 (indicated by red) the grafted thermoresponsive copolymer network exists in a collapsed and
889 highly charged state (top right) that affords high protein binding affinity. For elution a motor-
890 driven Peltier cooling device, the travelling cooling zone or TCZ (shown as a turquoise ring),
891 is moved along the column's full length at a velocity (v_c) lower than that of the mobile phase.
892 Within the cooled zone (shown in blue) generated by the TCZ travels along the column, the
893 tethered thermoresponsive copolymer expands, the charge density drops (bottom right) and
894 bound protein detaches from the support surfaces and is carried away in the exiting mobile
895 phase. For more details the reader is referred to sections 2.3, 3.1 and 3.3 of the text.

896

897 **Fig. 2.** Schematic illustrations of single protein loading (top) and concentration (bottom)
898 profiles at different stages during TCZR operation. The profiles correspond to three discrete
899 z/z_0 positions (<0, 0.25, 0.75) of the TCZ illustrated by the gray shaded vertical bars, i.e.: (i)
900 parked outside the separation column resulting in conventional operation with slowly
901 progressing concentration and loading profiles; (ii) shortly after initiation of TCZ movement,
902 where a sharp concentration peak evolves just ahead of the TCZ; and (iii) as the TCZ nears
903 the end of its journey along the column. At this point, in addition to further protein
904 accumulation within the elution peak, new loading and concentration profiles arising from
905 constant feed flow at the column inlet become clearly visible.

906

907 **Fig. 3.** FT-IR spectra during the fabrication of thermoCEX-S6pg supports (B1-B4)
908 characterized in Table 2. All spectra are normalized for peak height at the 'fingerprint'

909 wavenumber for agarose of 930 cm^{-1} characteristic of 3,6 anhydro moiety [28], and functional
910 groups expected of cross-linked agarose [23,28] are identified on the spectrum for Superose 6
911 Prep Grade.
912
913 **Fig. 4.** Optical transmittance (500 nm) vs. temperature profiles for 0.5% (w/v) solutions of
914 ungrafted free poly(NIPAAm-*co*-tBAAm-*co*-AAc-*co*-MBAAm) arising during fabrication of
915 (a) Sepharose CL-6B and (b) Superose based thermoCEX supports (detailed in Tables 1 and
916 2), and (c) the influence of NIPAAm content on temperature transition behaviour of the
917 copolymers. The symbols in 'c' indicate the determined LCST values at 50% transmittance
918 ($T_{50\%}$), capped bars define the temperature range over which phase transition occurred, and
919 the lower dotted and upper dashed lines respectively delineate the temperatures at which full
920 collapse ($T_{0.4\%}$) and extension ($T_{90\%}$) of the copolymer chains occurred. Key: pNIPAAm (★);
921 Sepharose CL6B series (A1 – □, A2 – ○, A3 – △, A4 – ▽); Superose series (B1 – ■, B2 –
922 ●, B3 – ▲, B4 – ▼, C1 – ●).
923
924 **Fig. 5.** Effect of temperature on the maximum adsorption capacity (q_{max}) of LF on (a)
925 thermoCEX-CL-6B supports (open circles) and (b) thermoCEX-S6pg (filled black circles)
926 and thermoCEX-S12pg (filled gray circles). The asterisks next to supports 'A2', 'B2' and
927 'C1' indicate those initially selected for TCZR chromatography (Fig. 7). The solid lines
928 represent linear fits to the data.
929
930 **Fig. 6.** Equilibrium isotherms for the adsorption of LF to thermoCEX supports initially
931 selected for TCZR chromatography (Fig. 7) 'A2' (a), 'B2' (b) and 'C1' (c) at 10, 20, 35 and
932 50 °C. The solid lines through the data points represent fitted Langmuir curves with parameter
933 values presented in Table 3.
934

935 **Fig. 7.** Chromatograms arising from TCZR tests conducted with thermoCEX supports 'A2'
936 (a), 'B2' (b) and 'C1' (c), employing multiple movements of the TCZ at a velocity, v_c, of 0.1
937 mm/s. Columns were saturated with LF (c_f = 2 mg/mL) and washed at the binding
938 temperature (35°C) prior to initiating the first of eight (a & b) or twelve (c) sequential
939 movements of the TCZ. Unshaded regions indicate column operation at a temperature of 35
940 °C with the TCZ in its 'parked' position. Gray shaded zones indicate the periods when the
941 TCZ moves along the column. The solid and dashed lines represent the absorbance and
942 conductivity signals respectively.
943
944 **Fig. 8.** Chromatograms arising from TCZR tests conducted with thermoCEX support 'B2'
945 employing eight movements of the TCZ at a velocity, v_c, of 0.1 mm/s. The columns were
946 continuously supplied with LF at concentrations c_f of (a) 0.5 mg/mL and (b) 1.0 mg/mL.
947 Unshaded regions indicate column operation at a temperature of 35 °C with the TCZ 'parked'.
948 Gray shaded zones indicate the periods when the TCZ moves along the column. The solid and
949 dashed lines represent the absorbance and conductivity signals respectively.
950
951 **Fig. 9.** Chromatogram arising from TCZR test conducted with thermoCEX support 'B2'
952 during continuous feeding of a binary protein mixture (1 mg/mL LF + 1 mg/mL BSA) and
953 movement of the TCZ at a velocity, v_c, of 0.1 mm/s. Unshaded regions indicate column
954 operation at a temperature of 35 °C with the TCZ 'parked'. Gray shaded zones indicate the
955 periods when the TCZ moves along the column. The solid and dashed lines represent the
956 absorbance and conductivity signals respectively. SDS-PAGE analysis of pooled flowthrough
957 (*a, c, e, g, i, k, m, o & q);* peak (*b, d, f, h, j, l, n & p*) and salt-stripped (S) fractions are shown
958 in Fig. 10.
959

960 **Fig. 10**. Reducing SDS 15% (w/v) polyacrylamide gel electrophoretogram corresponding to
961 the chromatogram shown in Fig. 9. Key: molecular weight markers (M); feed (F);
962 flowthrough fractions (*a, c, e, g, i, k, m, o & q);* peak fractions (*b, d, f, h, j, l, n & p*); and salt-
963 stripped fraction (S).
964

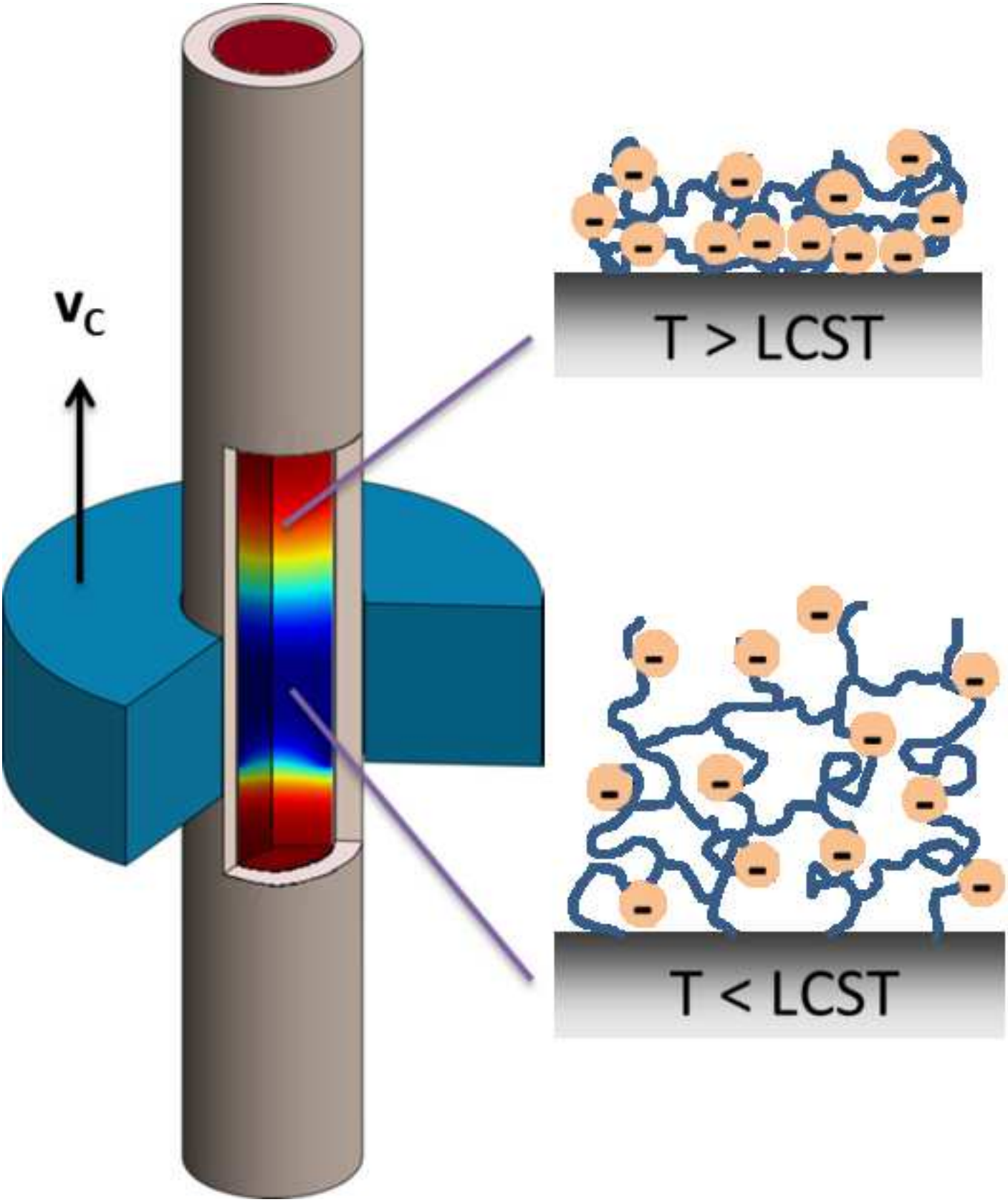

Figure 2

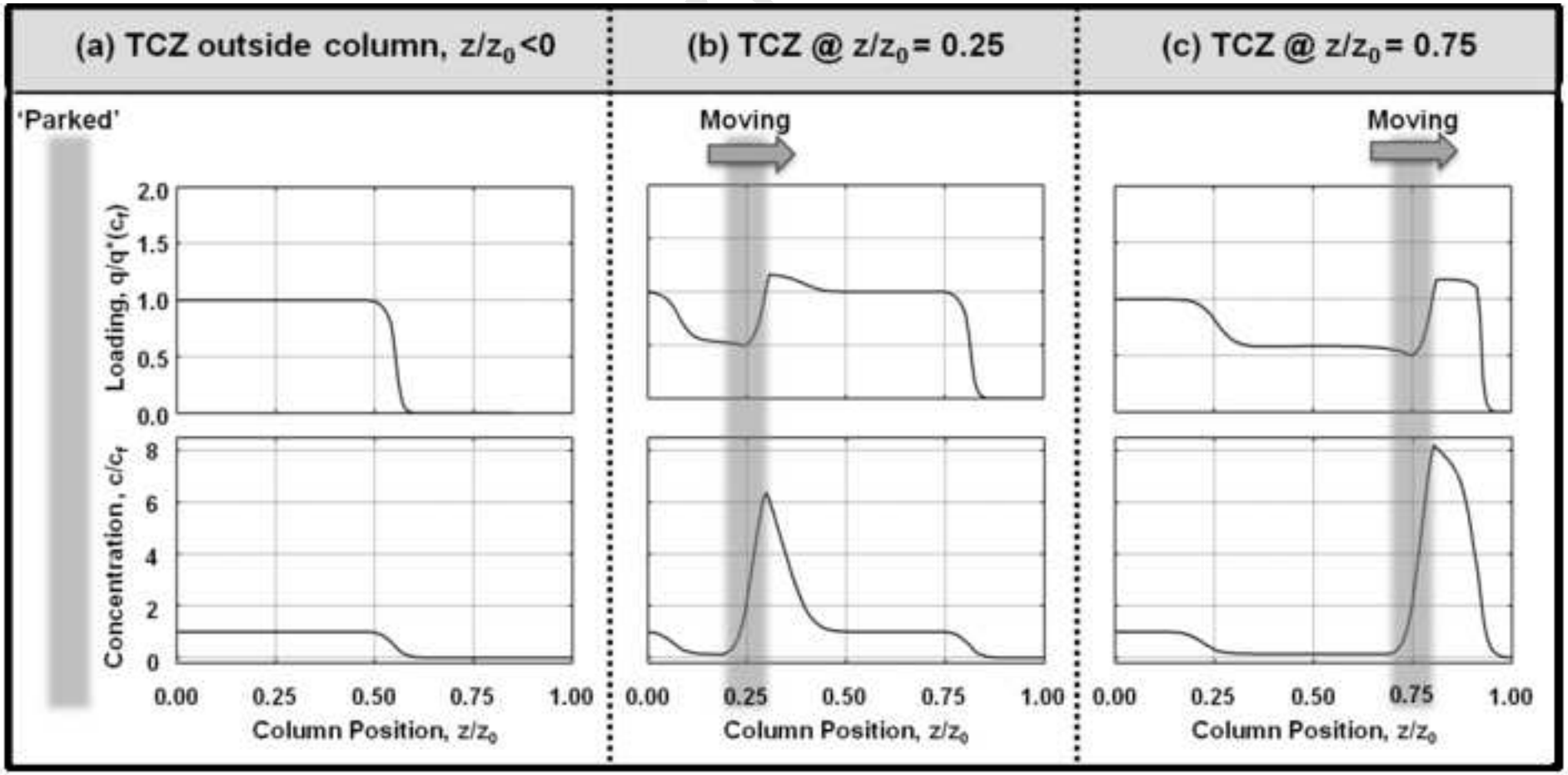
(a) TCZ outside column, z/z0<0
(b) TCZ @ z/z0= 0.25
(c) TCZ @ z/z0= 0.75
'Parked'
Moving
Moving
Loading, q/q*(cf)
Concentration, c/cf
Column Position, z/z0
Column Position, z/z0
Column Position, z/z0

Figure 3

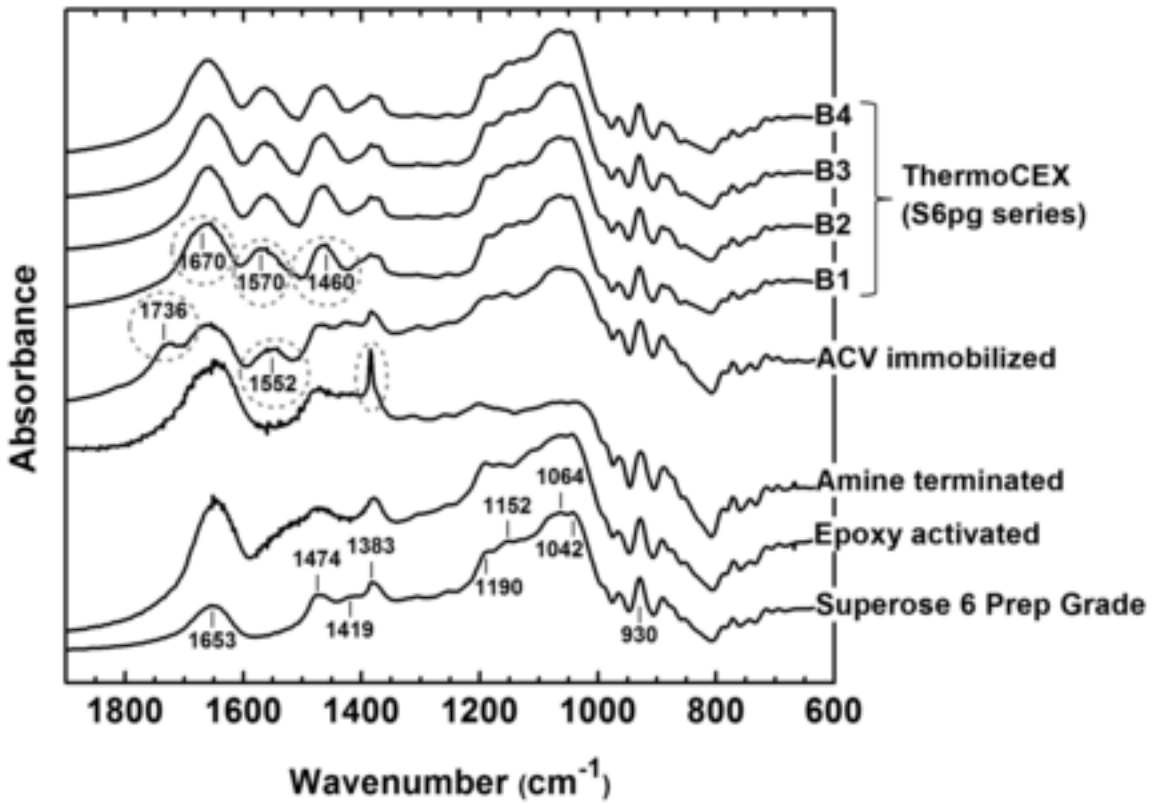
B4
B3
B2
B1
ThermoCEX
(S6pg series)
ACV immobilized
Amine terminated
Epoxy activated
Superose 6 Prep Grade
1670
1570
1460
1736
1552
1064
1152
1042
1474
1383
1190
1653
1419
930
Absorbance
1800
1600
1400
1200
1000
800
600
Wavenumber (cm-1)

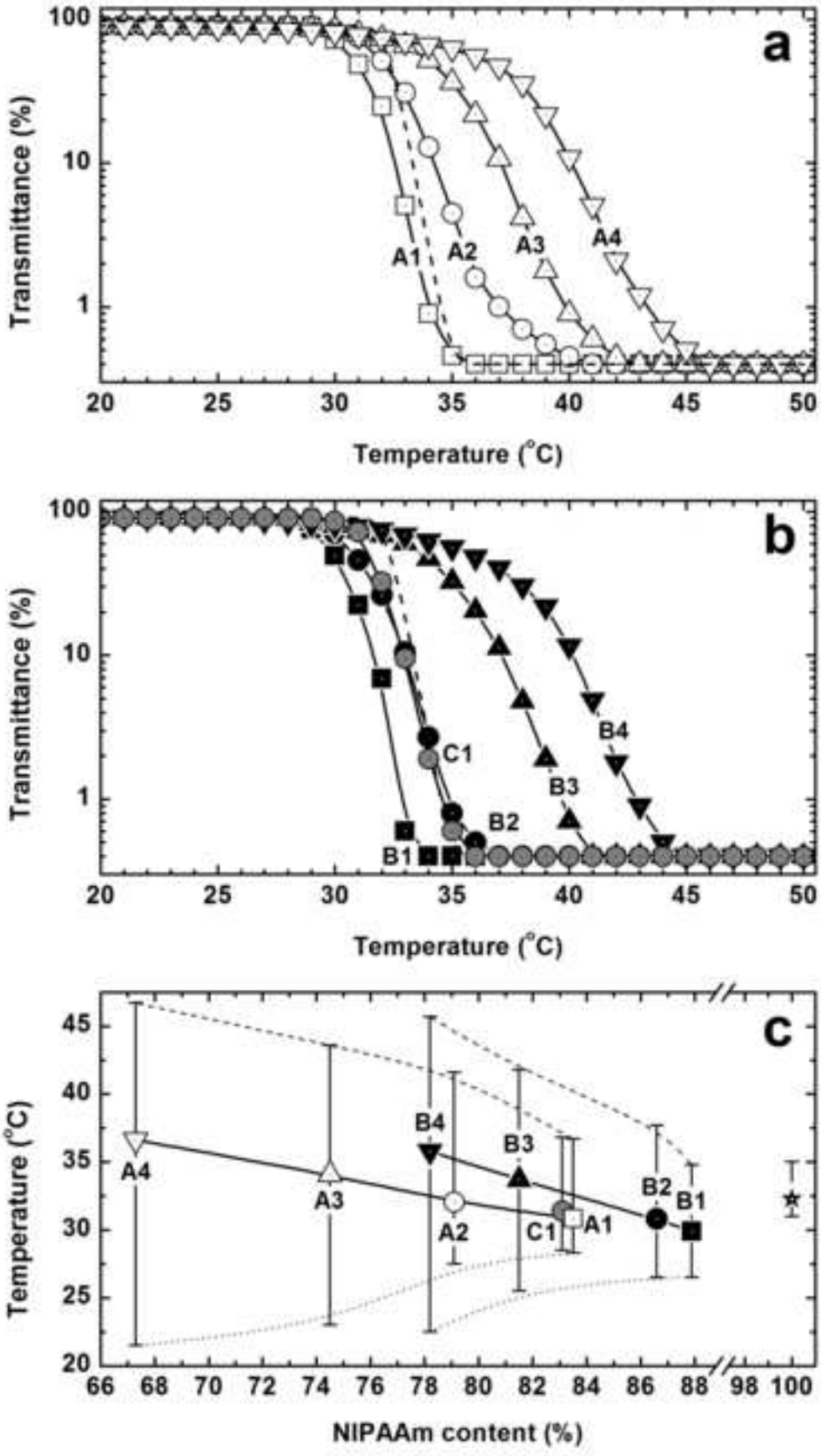

Figure 5

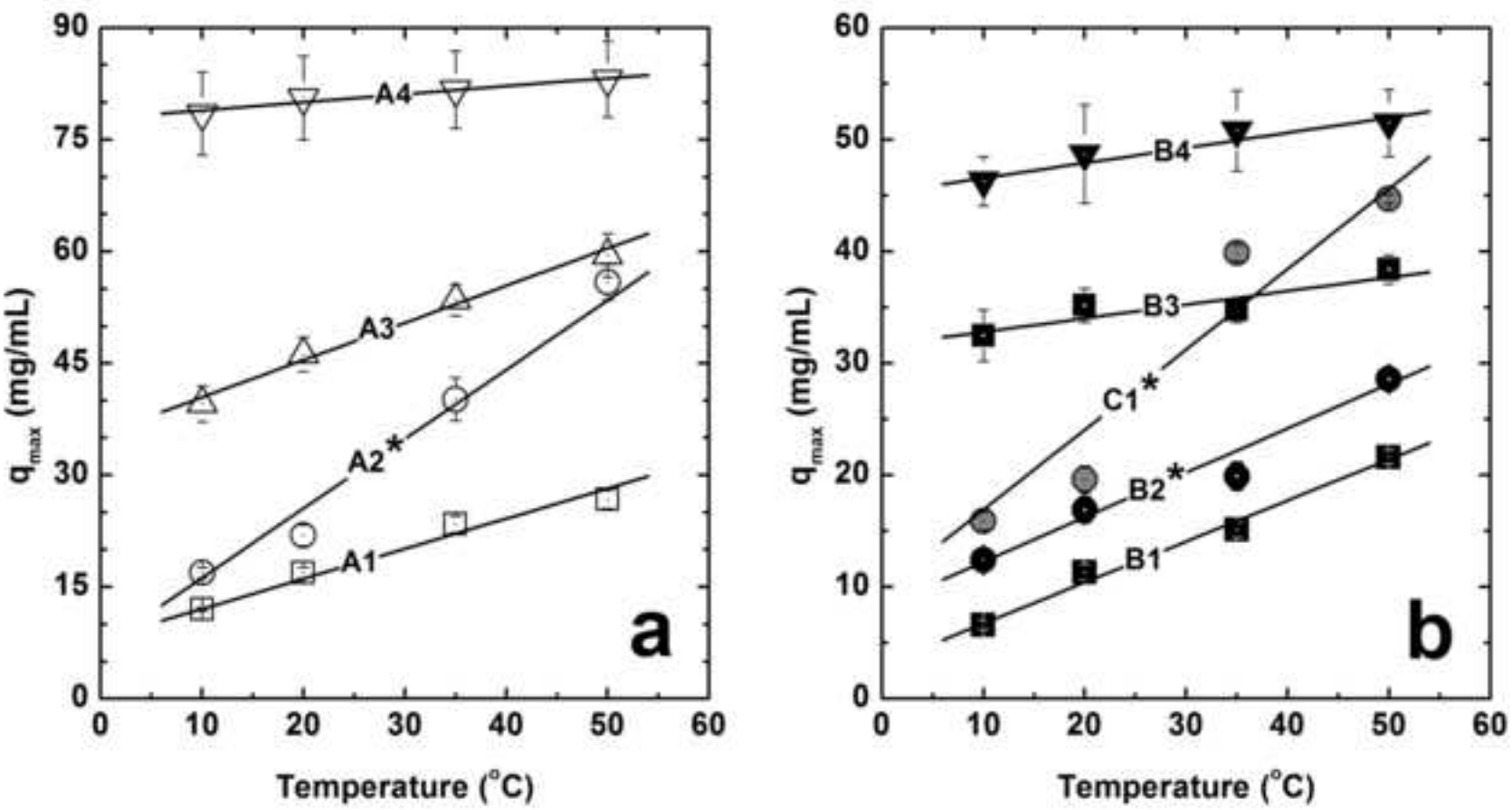
90
75
60
45
30
15
0
0
10
20
30
40
50
60
q_{max} (mg/mL)
Temperature (°C)
A4
A3
A2*
A1
a
60
50
40
30
20
10
0
0
10
20
30
40
50
60
q_{max} (mg/mL)
Temperature (°C)
B4
B3
C1*
B2*
B1
b

Figure 6

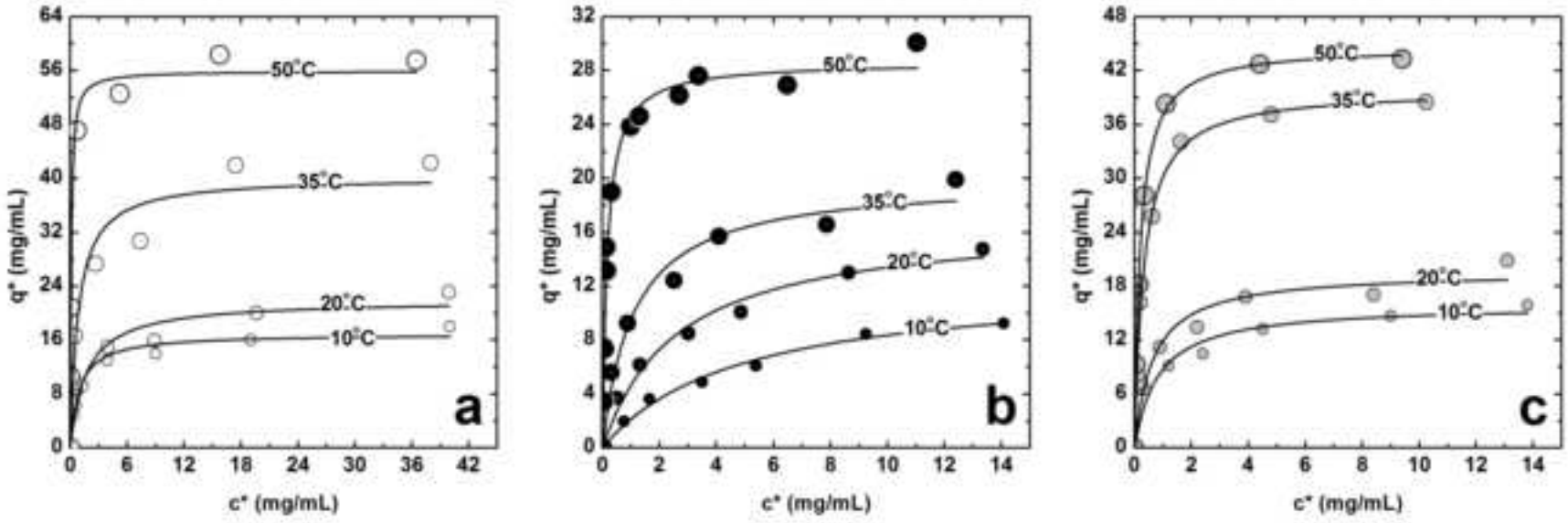

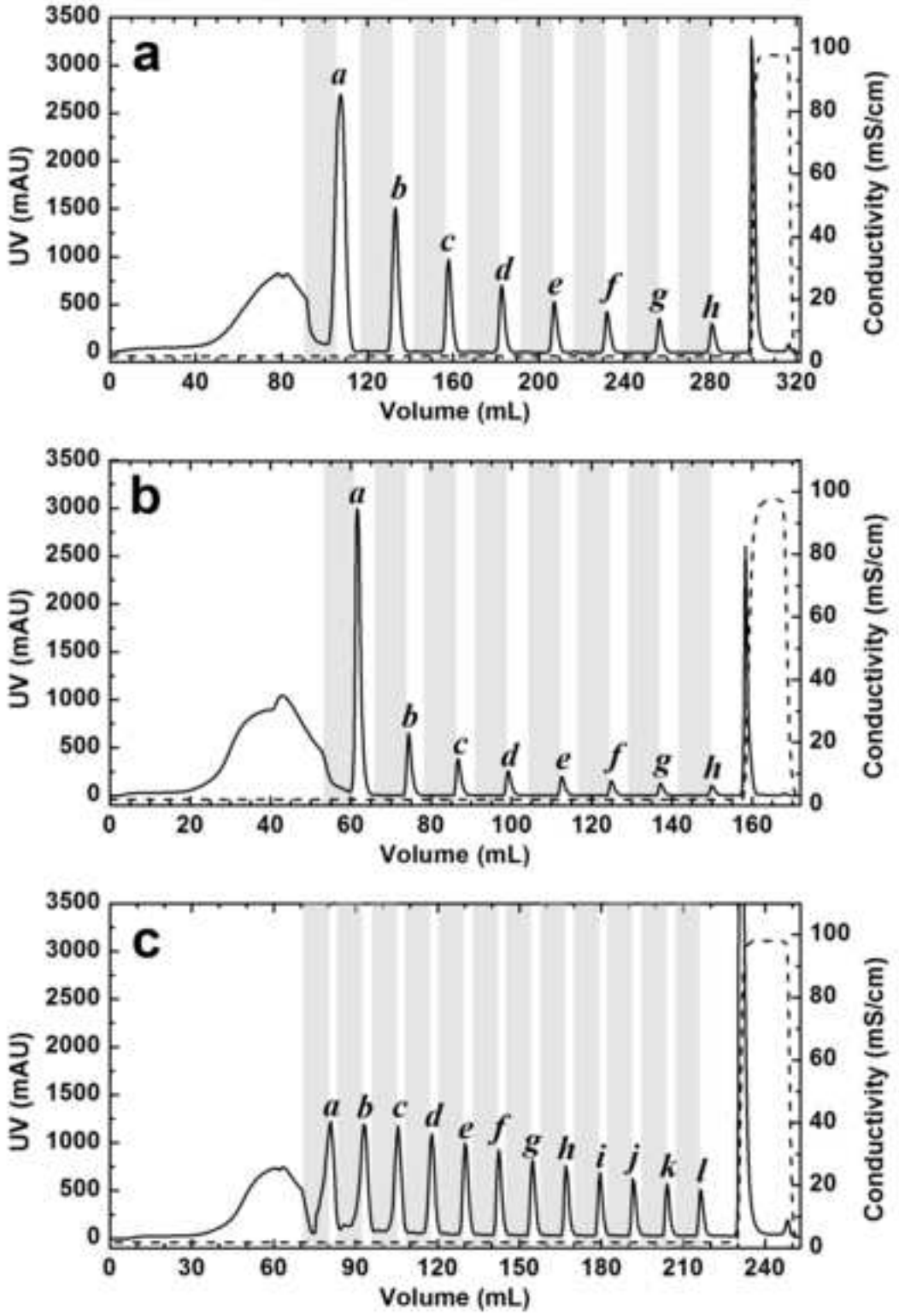

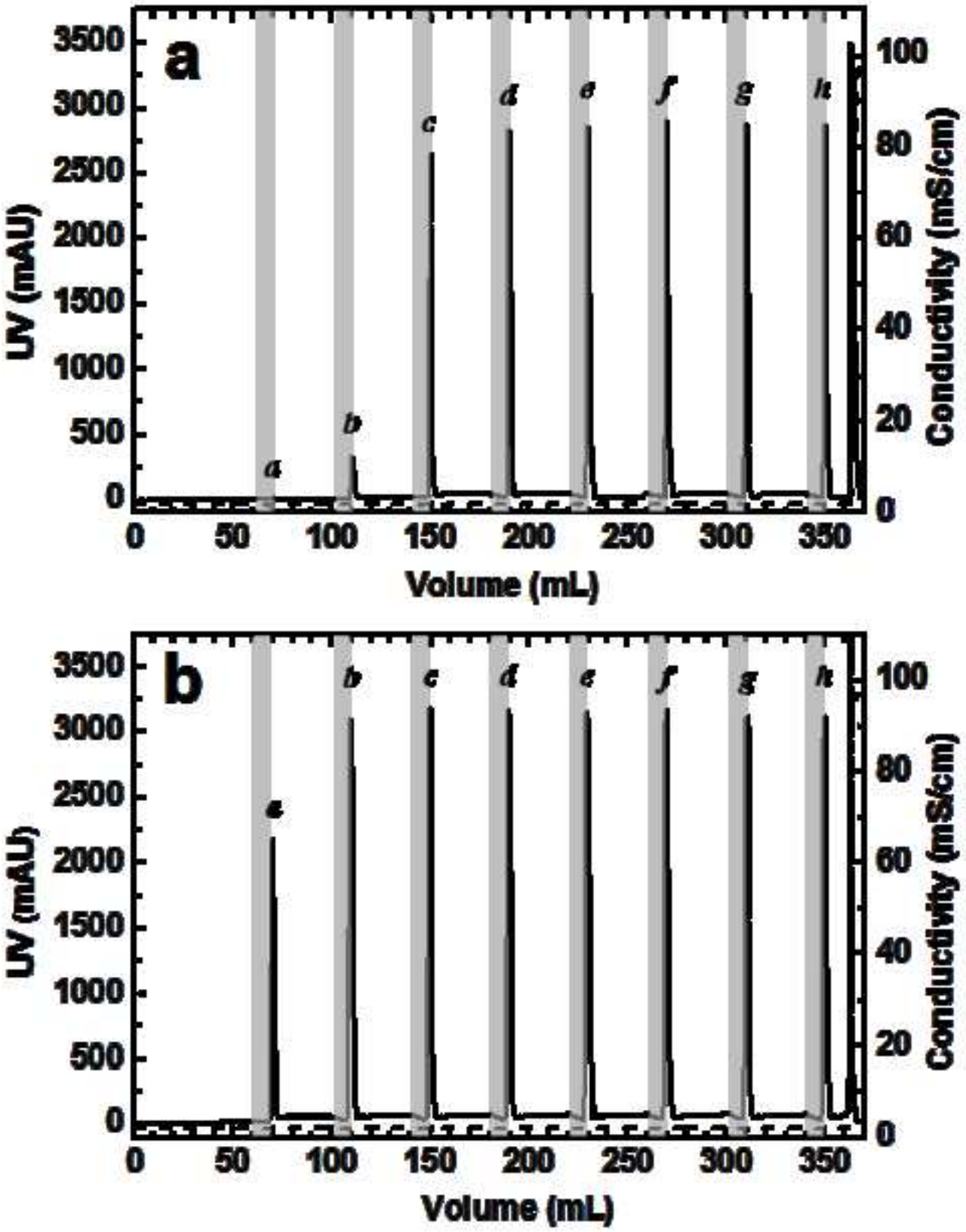

Figure 9

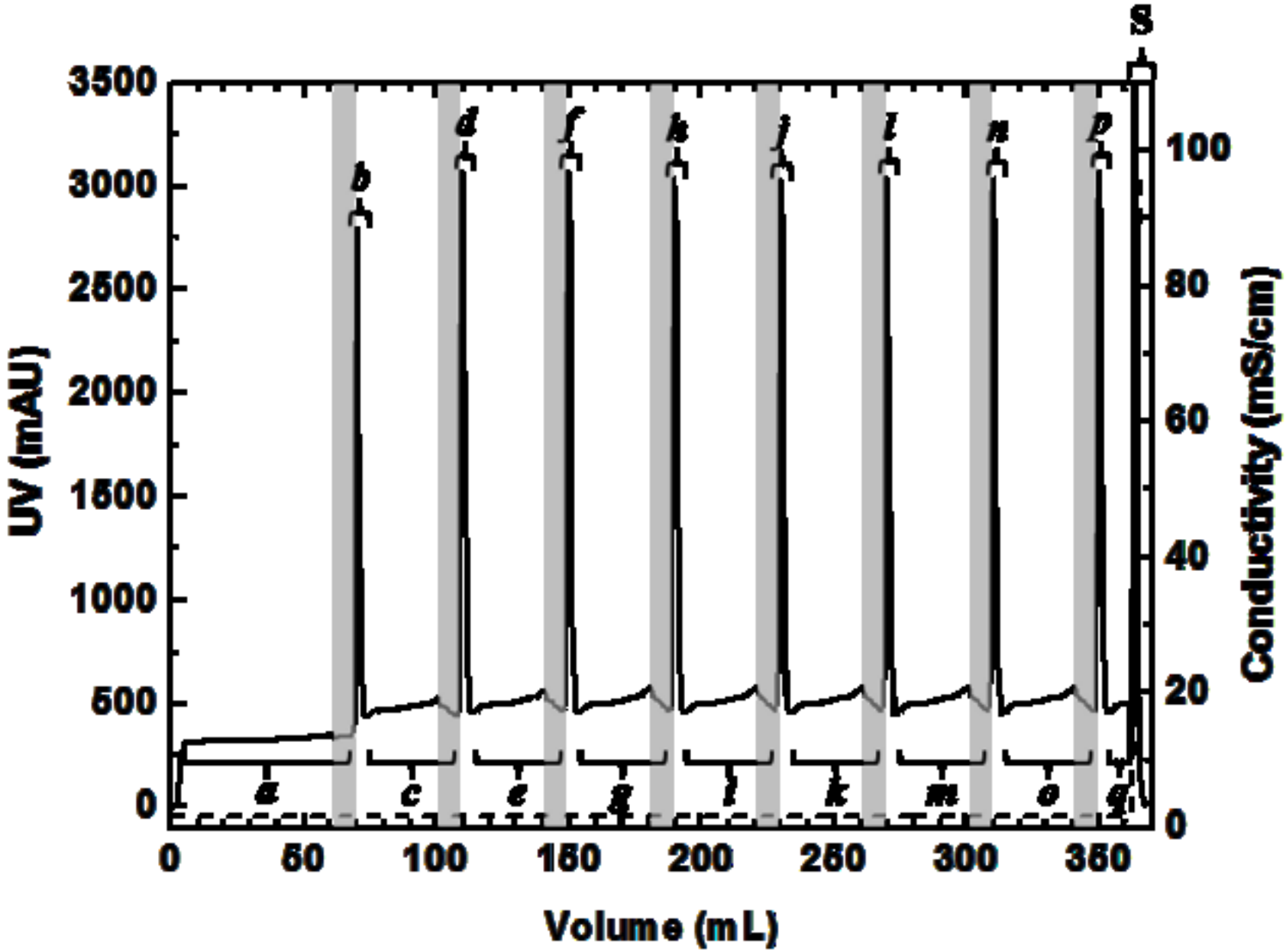
S
3500
3000
2500
2000
1500
1000
500
0
UV (mAU)
b
d
f
h
j
l
n
p
100
80
60
40
20
0
Conductivity (mS/cm)
a
c
e
g
i
k
m
o
q
0
50
100
150
200
250
300
350
Volume (mL)

Figure 10

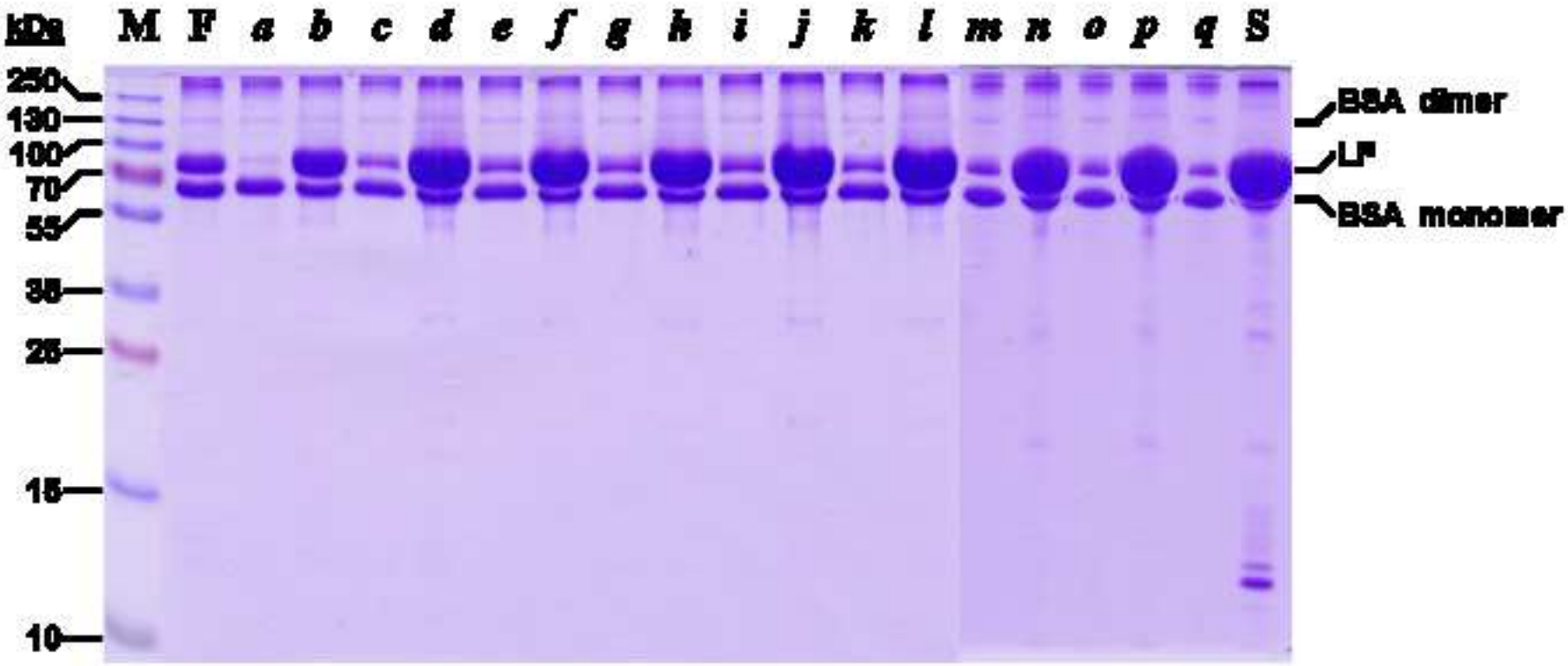
kDa
M
F
a
b
c
d
e
f
g
h
i
j
k
l
m
n
o
p
q
S
250
130
100
70
55
35
25
15
10
BSA dimer
LF
BSA monomer

Table 1. Characterization of the Sepharose CL6B based thermoCEX supports prepared and used in this work. See text for details.

Parameter	ThermoCEX-CL-6B			
Support ID	A1	A2	A3	A4
Base matrix	Sepharose CL-6B (lot 10061497)			
Particle size distribution	45 – 165 μm (98%)			
Globular protein fractionation range, M_r	$1 \times 10^4 – 4 \times 10^6$ Da			
Step 1. Immobilized oxirane content (μmol/g dried support) [a]	662			
Step 3. Immobilised ACV content (μmol/g dried support) [b]	380			
Step 4. Free monomers entering reaction:				
'NIPAAm:tBAAm:AAc' (mM)	900:50:25	900:50:50	900:50:100	900:50:150
'NIPAAm:tBAAm:AAc' ratio	90:5:2.5	90:5:5	90:5:10	90:5:15
Immobilized copolymer composition of thermoCEX support:				
'NIPAAm + tBAAm' content (μmol/g dried support) [b,c]	4227	4177	4131	3974
'NIPAAm:tBAAm' ratio [d]	90:10	88:12	85:15	81:19
NIPAAm content (μmol/g dried support)	3804	3676	3511	3219
tBAAm content (μmol/g dried support)	423	501	620	755
Ion exchange capacity (μmol H^+/g dried support) [e]	330	469	582	811
'pNIPAAm + tBAAm + AAc' content (μmol/g dried support)	4557	4646	4713	4785
'NIPAAm:tBAAm:AAc' ratio	83.5:9.3:7.2	79.1:10.8:10.1	74.5:13.2:12.3	67.3:15.8:16.9
% monomer consumed by support:				
NIPAAm + tBAAm + AAc	15.1	15.0	14.5	14.1
NIPAAm	13.7	13.2	12.6	11.6
tBAAm	27.4	32.5	40.2	49.0
AAc	42.8	30.4	18.9	17.5

Key: Determined by: [a]oxirane ring opening reaction followed by titration [25]; [b]gravimetric measurement; [c]ATR-FTIR spectrometry of supernatant samples before and after polymerization reactions, [d]Proton NMR of the ungrafted free copolymer in $CDCl_3$; [e]titration.

Table 2. Characterization of the Superose 6 and 12 based thermoCEX supports prepared and used in this work. See text for details.

Parameter	ThermoCEX-S6pg				ThermoCEX-S12pg
Support ID	B1	B2	B3	B4	C1
Base matrix	Superose 6 Prep Grade (lot 10037732)				Superose 12 Prep Grade (lot 10057699)
Particle size distribution	20 – 40 μm (83%)				20 – 40 μm (88%)
Globular protein fractionation range, M_r	$5 \times 10^3 – 5 \times 10^6$ Da				$1 \times 10^3 – 3 \times 10^5$ Da
Step 1 Immobilized oxirane content (μmol/g dried support) [a]	878				1018
Step 3. Immobilised ACV content (μmol/g dried support) [b]	568				611
Step 4. Free monomers entering reaction:					
'NIPAAm:tBAAm:AAc' (mM)	900:50:25	900:50:50	900:50:100	900:50:150	900:50:50
'NIPAAm:tBAAm:AAc' ratio	90:5:2.5	90:5:5	90:5:10	90:5:15	90:5:5
Immobilized copolymer composition of thermoCEX support:					
'NIPAAm + tBAAm' content (μmol/g dried support) [b,c]	5745	5733	5659	5641	5495
'NIPAAm:tBAAm' ratio [d]	92:8	91:9	87:13	84:16	89:11
NIPAAm content (μmol/g dried support)	5285	5217	4923	4738	4891
tBAAm content (μmol/g dried support)	460	516	736	903	604
Ion exchange capacity (μmol H^+/g dried support) [e]	268	293	382	416	391
'NIPAAm + tBAAm + AAc' content (μmol/g dried support)	6013	6026	6041	6057	5886
'NIPAAm:tBAAm:AAc' ratio	87.9:7.6:4.5	86.6:8.5:4.9	81.5:12.2:6.3	78.2:14.9:6.9	83.1:10.3:6.6
% monomer consumed by support:					
NIPAAm + tBAAm + AAc	19.9	19.5	18.6	17.8	19.1
NIPAAm	19.0	18.7	17.6	17.0	17.6
tBAAm	29.8	33.5	47.7	58.5	39.2
AAc	34.8	19.0	12.4	9.0	25.4

Key: Determined by: [a]oxirane ring opening reaction followed by titration [25]; [b]gravimetric measurement; [c]ATR-FTIR spectrometry of supernatant samples before and after polymerization reactions, [d]Proton NMR of the ungrafted free copolymer in $CDCl_3$; [e]titration.

Table 3. Langmuir parameters[a] describing the adsorption of LF at 10, 20, 35 and 50 ºC to three different thermoCEX media prepared under identical conditions using a common initial 'NIPAAm:tBAAm:AAc' ratio of '90:5:5' (Tables 1 & 2).

Support (ionic capacity)	Temperature (˚C)	q_{max} (mg/mL)	K_d (mg/mL)	Initial slope, q_{max}/K_d
thermoCEX-CL6B 'A2'	10	16.9 ± 0.7	0.93 ± 0.19	18.2
(40.7 μmol H^+/mL)	20	21.9 ± 1.4	1.66 ± 0.48	13.2
	35	40.2 ± 2.9	0.83 ± 0.34	48.4
	50	55.9 ± 2.4	0.09 ± 0.03	621.1
thermoCEX-S6pg 'B2'	10	12.4 ± 0.9	4.79 ± 0.83	2.6
(25.4 μmol H^+/mL)	20	16.9 ± 1.1	2.63 ± 0.52	6.4
	35	19.9 ± 1.2	1.09 ± 0.26	18.3
	50	28.6 ± 0.7	0.17 ± 0.02	168.2
thermoCEX-S12pg 'C1'	10	15.9 ± 0.8	0.82 ± 0.20	19.39
(34.8μmol H^+/mL)	20	19.6 ± 1.2	0.65 ± 0.20	30.2
	35	39.9 ± 0.7	0.32 ± 0.03	124.7
	50	44.7 ± 0.4	0.21 ± 0.01	212.9

[a]Figure 5 adsorption data were fitted to the Langmuir model (Eq. (1)).

Table 4. LF contents in peaks *a* – *h* obtained following eight sequential movements of the cooling zone during continuous feeding of LF (c_f = 0.5 and 1 mg/mL) to a column filled with the thermoCEX-S6pg 'B2' matrix (see Table 2).

LF concentration in feed (mg/mL)	LF content (mg) in peak:							
	a	*b*	*c*	*d*	*e*	*f*	*g*	*h*
0.5	0.0	1.46	10.5	12.3	13.4	14.5	17.8	13.2
1.0	7.54	28.9	31.3	31.2	31.4	30.6	31.7	28.1